

# Characteristics of Lightning within Electrified Snowfall Events using Lightning Mapping Arrays

Christopher J. Schultz\*, Timothy J. Lang

*NASA Marshall Space Flight Center, Huntsville, AL, 35812*

Eric C. Bruning

*Department of Geosciences, Texas Tech University, Lubbock, TX, 79409-2101*

Kristin M. Calhoun

*Cooperative Institute for Mesoscale Meteorological Studies, and NOAA/OAR/National Severe Storms Laboratory,*

*Norman, OK, 73072*

Sebastian Harkema, Nathan Curtis

*Department of Atmospheric Science, the University of Alabama-Huntsville, Huntsville, AL, 35805*

---

\* Corresponding author address: Dr. Christopher J. Schultz, NASA MSFC, Huntsville AL, 35812.  
Email: christopher.j.schultz@nasa.gov

## ABSTRACT

This study examined 34 lightning flashes within four separate thundersnow events derived from lightning mapping arrays (LMAs) in northern Alabama, central Oklahoma, and Washington DC. The goals were to characterize the in-cloud component of each lightning flash, as well as the correspondence between the LMA observations and lightning data taken from national lightning networks like the National Lightning Detection Network (NLDN). Individual flashes were examined in detail to highlight several observations within the dataset.

The study results demonstrated that the structures of these flashes were primarily normal polarity. The mean area encompassed by this set of flashes is  $375 \text{ km}^2$ , with a maximum flash extent of  $2300 \text{ km}^2$ , a minimum of  $3 \text{ km}^2$ , and a median of  $128 \text{ km}^2$ . An average of 2.29 NLDN flashes were recorded per LMA-derived lightning flash. A maximum of 11 NLDN flashes were recorded in association with a single LMA-derived flash on 10 January 2011. Additionally, seven of the 34 flashes in the study contain zero NLDN identified flashes. Eleven of the 34 flashes initiated from tall human-made objects (e.g., communication towers). In at least six lightning flashes, the NLDN detected a return stroke from the cloud back to the tower and not the initial upward leader. This study also discusses lightning's interaction with the human built environment and provides an example of lightning within heavy snowfall observed by GOES-16's Geostationary Lightning Mapper.

## 1. Introduction

Lightning and thunder during snowfall (i.e., “thundersnow”) is a phenomenon that is correlated to heavy snowfall rates [e.g., *Crowe et al.*, 2006; *Pettegrew et al.*, 2009; *Market and Becker*, 2009]. *Schultz and Vavrik*, [2009] describe the ingredients necessary for lightning to occur in snowfall, and state that all thundersnow events are considered convective because they have strong enough vertical motion to separate charge to produce lightning. Previous thundersnow studies used observations from surface or upper-air stations [e.g., *Market et al.*, 2002; *Market et al.*, 2006] or characteristics of cloud-to-ground (CG) lightning behavior of these events from networks like the National Lightning Detection Network [NLDN, *Orville*, 2008; *Cummins and Murphy*, 2009; *Buck et al.*, 2014]. This is primarily due to the availability of the data and the spatial/temporal coverage of these networks [e.g., *Schultz*, 1999; *Trapp et al.*, 2001, *Dolif Neto et al.*, 2009; *Market and Becker*, 2009; *Pettegrew et al.*, 2009; *Steiger et al.*, 2009; *Warner et al.*, 2014]. These studies found that flashes of both polarity occur within electrified snowfall, lightning typically accompanies the highest snowfall rates within the storm, and many of the CG flash locations were found 15-50 km *outside* of the heaviest precipitation bands [e.g., *Pettegrew et al.*, 2009; *Market and Becker*, 2009; *Warner et al.*, 2014].

The literature includes very few measurements of the in-cloud component during such events [e.g., *Takeuti et al.*, 1978; *Brook et al.*, 1982; *Michimoto*, 1993; *Kitagawa and Michimoto*, 1994; *Kumjian and Deierling*, 2015]. Most of these studies observed strong positive flashes from the same region along the Sea of Japan [e.g., *Takeuti et al.*, 1978; *Brook et al.*, 1982; *Michimoto*, 1993; *Kitagawa and Michimoto*, 1994]. *Kuhlman and Manross*, [2011], *Schultz et al.*, [2011], and *Kumjian and Deierling*, [2015] were the only studies out of this group to present the total lightning characteristics using lightning mapping array technology [LMA; *Rison et al.*, 1999; *Krehbiel et*

69 *al.*, 2000]. *Kuhlman and Manross*, [2011] and *Kumjian and Deierling*, [2015] focused on radar  
70 observables at the time of winter lightning flashes. *Kuhlman and Manross*, [2011] observed that  
71 the lightning produced in one event was located at a transition zone between liquid precipitation,  
72 sleet<sup>1</sup>, and snow as observed by polarimetric radar. *Kumjian and Deierling* [2015] observed that  
73 most thundersnow events in Colorado occurred in convective cells that contain graupel and pristine  
74 ice. Furthermore, their comparison of lightning- and non-lightning-producing cells revealed that  
75 the lightning-producing cells had larger specific differential phase values ( $K_{dp}$ ), implying more  
76 supercooled liquid water and larger ice masses. *Thompson et al.* [2014] indicated that these  $K_{dp}$   
77 signatures were most likely the result of dendritic growth. Additional observations from electric  
78 field meter (EFM) balloon flights in *Rust and Trapp* [2002] showed an electric field maximum  
79 within the bright band in electrified winter nimbostratus, and noted a normal dipole (positive above  
80 negative charge) near the surface when the melting layer was near the ground; however, no  
81 lightning was observed within 100 km of their balloon flights.

82         Several authors have also shown that lightning flashes within winter storms were  
83 clustered near tall human-made objects such as communications towers and wind turbines [e.g.,  
84 *Schultz et al.*, 2011; *Bech et al.*, 2013; *Warner et al.*, 2014]. *Schultz et al.*, [2011] presented four  
85 lightning flashes within thundersnow events that initiated from tall communications towers using  
86 the North Alabama and Washington, DC LMAs. They also used their analysis to compare several  
87 winter CG flashes observed at tall buildings and communications towers near Chicago, IL on 1-2  
88 February 2011. *Bech et al.*, [2013] noted that multiple CG strokes clustered near communications  
89 towers during a crippling winter storm in northeastern Spain. *Warner et al.*, [2014] examined the  
90 1-2 February 2011 blizzard near Chicago, IL in greater detail and found that a large majority of

---

<sup>1</sup> A type of precipitation consisting of transparent or translucent pellets of ice, less than 5 mm in diameter formed by the freezing of raindrops or refreezing of large aggregate snowflakes that have melted (AMS Glossary, 2012).

flashes were found at the locations of communications towers, wind turbines and tall buildings during this event, providing ample evidence of the interaction between human-made structures and lightning in winter storms.

While there is a fairly good understanding of the ground flash component of flashes in electrified snowfall, there has been very little study of the spatial characteristics of the in-cloud components of flashes in these systems. Furthermore, these studies have not illustrated the detailed spatial and temporal relationships between the in-cloud (IC) and CG components in these flashes, specifically the correspondence between different lightning datasets that observe the same lightning event (e.g., LMA vs. NLDN). Detailed analyses of flash sizes, charge structure or leader propagation patterns within these storms have not been largely performed in winter events.

Therefore, the purpose of this paper is to make full use of the LMA data to show the observed development patterns of these flashes and expand upon the work of *Schultz et al.*, [2011]. The present study will characterize lightning within four thundersnow storm events that were within the range of LMAs. Examination of each flash's charge structure, two-dimensional footprint, and of number of NLDN flash detections per LMA-derived flash are presented. The characterization of the spatial extent of lightning flashes within electrified snowfall events is vital for fundamental understanding of how lightning data can be utilized for short-term decisions (< 30 minutes). Furthermore, the spatial characteristics from the LMA coupled with the NLDN measurements provide insight into the utility of total lightning observations from the Geostationary Operational Environmental Satellite (GOES)-16's Geostationary Lightning Mapper [GLM; *Goodman et al.*, 2013] to monitor hazardous winter weather conditions.

## 2. Data and Methodology

### 2.1 Lightning Data

#### *a. Lightning Mapping Array (LMA) Data*

Observations from very high frequency (VHF) LMA networks in Northern Alabama [NALMA; *Koshak et al.*, 2004], Washington, D.C. [DCLMA; *Krehbiel*, 2008] and Central OK [OKLMA; *MacGorman et al.*, 2008] were used to analyze lightning flashes in winter storms. A minimum of 7 LMA stations were required to detect and locate the VHF sources, and the source location needed a chi-squared value  $\leq 1.0$  for it to be considered valid for use in this analysis. This 7-station requirement and chi-squared threshold provided a more accurate VHF source location, which was important in determining flash size [*Bruning and Thomas*, 2015]. VHF LMA source points were grouped using space and time criteria into flashes using the algorithm of *Thomas et al.*, [2004]. The space and time criteria used for combining two VHF source points is 3000 m in the horizontal, 5000 m in altitude, and 150 ms in time. A minimum of 10 VHF sources were required to identify a flash in order to eliminate spurious noise points.

#### *b. National Lightning Detection Network (NLDN) data*

CG lightning information was obtained from the NLDN [*Cummins and Murphy*, 2009; *Buck et al.*, 2014]. NLDN flash and stroke data were examined to determine if flashes contained single or multiple lightning strokes as well as determine the flash's location with respect to tall objects like communications towers. The NLDN detects 90-95% of all CG lightning and has a median spatial error of 500 m [*Cummins and Murphy*, 2009; *Buck et al.*, 2014]. All flashes with peak amplitudes between (and not including) -10 and +15 kA were considered intracloud (IC) flashes following the guidance of *Biagi et al.*, [2007] and *Fleenor et al.*, [2009]. NLDN stroke-

level data were also utilized to assess stroke polarity in flashes with multiplicities greater than 1 and in the identification of potential tower-initiated flashes.

### *c. Geostationary Lightning Mapper (GLM) Data*

One example of GLM data is provided within this work to demonstrate the capability of the GLM instrument aboard the GOES-16 satellite in electrified snowfall events [Goodman *et al.*, 2013]. The GLM instrument is a 1372 x 1300 pixel charge coupled device (CCD) that is in the geostationary orbit GOES-East Position of 75°W longitude. The instrument detects emission from lightning in the 777.4 nm band, which allows for detection of lightning both during the day and at night. The nadir resolution of the instrument is 8 km by 8 km, with a resolution of ~9 km by 14 km at the edges of the field of view.

At the present time there are 3 baseline products developed from the GLM information. These are GLM events, GLM groups, and GLM flashes [Goodman *et al.*, 2012]. A GLM event is defined as the occurrence of a GLM single pixel exceeding the instrument background threshold during a 2 ms period. A GLM group is defined the grouping of one or more simultaneous GLM events that occur in the same 2 ms period and that are adjacent to each other. A GLM flash is then defined as a set of GLM groups that are sequentially separated in time by no more than 330 ms and 16.5 km. The reported position of the GLM flash is the space averaged location of all of the GLM groups that make the flash. Similarly, the GLM group location is the space averaged location of all of the GLM events that make up the GLM group. Therefore, in order to accurately depict spatial information from GLM, GLM events, groups, and flashes must be used in conjunction with each other to provide the maximum information possible when analyzing lightning from GLM.

d. *Integration of lightning data in this analysis*

The term “flash” is an arbitrary metric that is defined by the frequency range in which the measurement is being taken; thus, the definition is different across instrument platforms [Cummins and Murphy, 2009; Nag et al., 2015]. It is important to emphasize that flashes will be presented in the present work as “LMA-derived” or “NLDN-derived” because each lightning system does not observe the same processes of a lightning flash.

The LMA is referenced as the best detection capability of lightning events because the system observes >99% of all lightning activity within 50 km of the center of the LMA network and provides high resolution three-dimensional information on lightning as it occurs in the cloud [e.g., Rison et al., 1999; Koshak et al., 2004; Fuchs et al., 2016]. One large drawback the LMA is that each network is limited in range and the LMA’s detection of lightning drops off between 100-200 km from the center of the network [Koshak et al., 2004; Fuchs et al., 2016].

The main advantages of networks like the NLDN are large spatial coverage and accurate location of CG flashes [Buck et al., 2014; Nag et al., 2015]. The NLDN also provides IC flash information which helps in the interpretation of charge structures when combined with the LMA. The location of CG flashes is important because the LMA does not always detect the lowering of the leader to the ground, and GLM will not be able to reliably discern an IC flash from a CG flash because its detecting light that comes through cloud top. The main drawback of the NLDN is that there is very little areal information on lightning flashes because it is difficult to determine if two separate NLDN flashes are related in space and time in the NLDN data.

It is expected that multiple NLDN-derived flashes will be associated with one LMA-derived flash (and also GLM flash data once available). This is why the authors do not simply provide a single comparison of “flash rates” in each of the following snowfall events to determine

which lightning observation is superior. Thus, the reader should expect that the flash counts from the LMA and NLDN in the following examples (and in other lightning related works) are not always 1:1 because they do not detect the same lightning processes. This is why Bayesian approaches have been used to intercompare systems that observe different lightning processes [e.g., *Bitzer et al.*, 2016].

## **2.2. Flash Area Estimation**

The area of each flash in the study was defined using the convex hull approach of *Bruning and MacGorman*, [2013]. The convex hull polygon was defined by the minimum area that encompasses the plan projection of all VHF source points of each flash. The convex hull approach allowed for the flash to define the geometry instead of assuming a predetermined form (e.g., square or ellipse). The area inside the hull was used to estimate the flash area. The area of each flash was recorded in units of  $\text{km}^2$ . NLDN flashes that occurred within the spatial bounds of the convex hull and temporal length ( $\pm 1$  s) of the LMA flash were assigned to the LMA flash. The  $\pm 1$  s buffer was used because of temporal offsets between the LMA and NLND noted during the present analysis.

## **2.3 Leader Speed and Charge Structure Determination**

The LMA and NLDN data were utilized to assess the charge structure present at lightning occurrence to ascertain basic charge structures within the cloud at the time of the lightning flash [e.g., *Rison et al.*, 1999; *Weiss et al.*, 2008; *Kuhlman et al.*, 2009; *Bruning et al.*, 2012; *Lang et al.*, 2014]. Leader speeds derived from LMA measurements were important in diagnosing charge structure [e.g., *Montanyà et al.*, 2014; 2015]. Negative leader speeds have been observed to be closer to  $10^5 \text{ m s}^{-1}$ , while positive leader speeds have been observed to be closer to  $5 \times 10^4 \text{ m s}^{-1}$  [*Campos et al.*, 2014; *Montanyà et al.*, 2015]. Positive leaders propagate into negative charge,

while negative leaders propagate into positive charge [Rison *et al.*, 1999]. Therefore, the speed of the leader can help to infer the sign of the charge region the leader is propagating into during electrical breakdown.

To determine the leader speed a multiple step processes was developed to calculate leader speed. First, all VHF source points in an single LMA-derived flash were made relative to the time of the first VHF source of that same flash by differencing the time of each VHF source in the flash from the time of the first. Next, a scatter plot of time since flash initiation versus height of VHF source points were created to estimate the leader speed. In longer duration flashes, multiple vertical leaders can be identified; thus the leader speeds were visually isolated from the remaining parts of the flash as shown in Fig. 1A. In these instances, the time differencing was done relative to the first VHF source in the segment of interest. Green and blue lines representing  $10^4 \text{ m s}^{-1}$  and  $10^5 \text{ m s}^{-1}$  are then overlaid on the plots as references to the speed of the leader observed in each case presented below.

Furthermore, the sign in front of IC flashes detected by the NLDN can help identify which sign of the charge at the location of the NLDN flash. The positive and negative signs in front of the IC designation does not mean that the flash has that particular polarity because IC flashes inherently neutralize charge of both polarities within the cloud [MacGorman *et al.*, 2001]. However, -IC flashes identified by the NLDN illustrate when leader of the flash is propagating in negative charge, while the +IC flashes identify when the leader of the flash is in positive charge [Bruning *et al.*, 2014]. The polarity of CG flashes is also useful in helping to diagnose the overall charge structure of each lightning flash because the sign of the CG flash reflects the sign of the charge being transferred to the ground.

## 2.4. Thermodynamic Information

Vertical temperature profiles were obtained through two sources: upper-air soundings and model-output soundings from the Rapid Update Cycle [RUC; *Benjamin et al.*, 2004]. Model-output soundings were used when upper-air information was not available less than 3 hours prior to the observance of lightning. Vertical temperature and dew point profiles provided to show the bottom, the depth, and saturation of the atmosphere around the time of lightning occurrence. Low-level saturation within the atmosphere which is a key element for lightning in snowfall [e.g., *Schultz* 1999; *Market et al.*, 2006] because charge must be separated between ice crystals and hydrometeors like graupel in the presence of supercooled water [*Saunders et al.*, 2006]. *Emersic and Saunders*, [2010] showed in laboratory results that surface growth rates of ice crystals and charge separation was maximized between -10°C and -25°C in water saturated environments. In one event, the temperature data were overlaid on radar data to illustrate the location of temperature information within a microphysical environment.

## 3. Results

Thirty-four LMA-derived lightning flashes from four electrified snowfall events were examined in detail in this study. The four events were: 24 December 2009 near Norman, OK, 6 February 2010 near Baltimore, MD, 10 January 2011 near Huntsville, AL, and 26 January 2011 near Washington DC. Each event produced snowfall in excess of 15 cm over the entire duration of the event, and all of these flashes occurred in regions where snow was observed at the surface at the time of the flash. Nine of the 34 flashes were examined in detail below to characterize behavior of flashes within multiple electrified events. A summary of flash size, polarity and correspondence with NLDN information was generated for each of the 4 lightning-producing winter storms.

### 3.1. 10 January 2011, Huntsville, AL

The first flash of this event occurred at 04:31:26.10 UTC. The flash encompassed an area on the order of 2300 km<sup>2</sup>, had a major axis in the east-west direction of 90 km (furthest east VHF source point to furthest west VHF source point), and came to ground in 4 separate places (as identified by the NLDN) separated by tens of kilometers [Fig. 1]. Using the location of the first 10 VHF source points from the LMA, plus the NLDN and Google Earth imagery, the flash originated from a television communications tower located at latitude/longitude 34.710, -86.537 in Huntsville, AL. The upward propagation of the flash in the LMA was readily apparent by the vertical trail of early VHF source points emanating from the tower location [Fig. 1]. This vertical trail of VHF sources is similar to those observed in the literature where manmade structures initiate flashes [e.g., *Montanya et al.*, 2014]. A slight difference in timing of about 200 ms was noted between the upward progression of the first VHF source points from the LMA and the first NLDN identification of the flash at the tower location [Fig. 1]. Three very well-resolved upward negative leaders were seen in the LMA information at 04:31:27.20 UTC, 04:31:27.60 UTC and 04:31:28.20 UTC, with the polarity of the leaders confirmed by leader speed observations and return strokes in the NLDN observations [Figs. 1 and 2]. The LMA and NLDN indicate that the overall charge structure of this flash was positive charge over negative charge [Fig. 1, right]. The NLDN shows that this flash came to ground in 4 separate locations spanning a distance of approximately 60 km. All four ground flashes were negative with peak amplitudes of -79, -53, -35 and -10 kA. At least one of these locations was at an electrical power substation (34.706, -86.706) and a second was at the location of an electrical transmission line at latitude/longitude 34.576, -87.079. The final ground location was in an open field in Lawrence Co. Alabama. The remaining 7 -IC flashes

observed by the NLDN were located at the television communications tower (1 -IC flash) and the electrical transmission line (6 -IC flashes).

Figure 3 presents a more complex tower-initiated flash that occurred at 04:58:30.48 UTC, 10 January 2011. This flash initiated from the same communications tower as the first. Initially a positive leader propagated into a region of negative charge located between 2 and 4 km in altitude [Fig. 3A]. At 04:58:30.48 UTC a negative leader began at the 2 km level, propagated upward, and then descended while moving westward down to 2 km [Fig. 3A, green points]. A second negative leader propagated southward from its original location at 4 km in altitude, about 10 km to the southeast of the tower initiation point [Fig. 3A, yellow source points]. Positive leader propagation continued eastward into Jackson County, AL just prior to the initiation of a third negative leader at 04:58:31.70 UTC. This third negative leader began around 4 km in Jackson Co. and propagated upward to 8 km before terminating. In total the flash was 890 km<sup>2</sup>, and the NLDN<sup>2</sup> did not report any lightning activity in North Alabama at this time. The charge structure observed by the LMA was positive charge over negative charge for this flash [Fig. 3B].

A radiosonde launched from the University of Alabama-Huntsville at 0303 UTC on 10 January 2011, shows that both negative and positive charge regions were found at temperatures warmer than -10°C at 2.5 km, while in a deeper part of the storm (perhaps convective) the charge layers were above -10°C [Fig. 4]. The charge structure resembles a normal polarity dipole of positive charge over negative charge; however, individual channel paths suggest that sloping charge layers were present at the time of the second flash [Fig. 3B]. A range-height-indicator (RHI) of horizontal radar reflectivity from the University of Alabama-Huntsville's Advanced Radar for Meteorological and Operational Research [ARMOR; *Schultz et al.*, 2012; *Mecikalski et al.*, 2015]

---

<sup>2</sup> Lightning was also not observed at this location and time with the Earth Networks Total Lightning Network or the Worldwide Lightning Location Network.

C-Band polarimetric radar at 04:57:10 UTC shows that taller precipitation features were present downrange of the radar location. VHF source heights reached their maximum altitude of 7.5 km approximately 40-50 km down range from the radar in the taller precipitation features during the event [Fig. 4B]. In Fig. 4C the polarimetric variable correlation coefficient for the same RHI shows that the lightning flash primarily travels along gradients between regions with hydrometeor diversity [e.g., different shapes, sizes, orientations, and types of hydrometeors; yellow-orange color] and homogenous hydrometeors [same shapes, sizes, orientation, and types; maroon color]. Like the flash itself, these gradients were sloping upward from southwest to northeast into the deeper part of the storm.

An upward initiated flash produced a return stroke back at the point of initiation at 05:10:25.34 UTC in Huntsville, AL [Fig. 5]. During the early stages of the flash, there was a clear upward progression in the VHF source points from the location of the tower. The leader propagated in altitude to around 5 km and in a southeast direction from the tower location. Then at approximately 05:10:26.00 UTC, 7 VHF sources were noted to retrace the flash path back toward the tower location, with 1 VHF source *and* the NLDN negative CG stroke occurring at the communications tower location at the same time. This was evidence of a negative dart leader traveling back to the ground, retracing the path of the upward positive leader and then striking the tower.

### **3.2. 26 January 2011, Washington, DC**

This was a prolific snowfall event between 1900 UTC on 26 January 2011 and 0200 UTC on 27 January 2011. Up to 30 cm of snow fell during this period in a corridor from Northeast Virginia through East Central Maryland. Upper-air temperature and wind profiles from Sterling, VA (KIAD) and the Aberdeen Proving Ground (KAPG) in Loudon, MD at 1200 and 1800 UTC

were used to assess the vertical temperature profile evolution during this event [Fig. 6]. At 1200 UTC, both KIAD and KAPG show that the profile of temperature between the surface and 700 hPa (2.7 km above ground level) ranges between -2.9 and -0.3°C [Fig. 6a, c]. The wind profile is northeasterly from the surface to 850 hPa, and then southwesterly from 850 to 100 hPa. Another upper-air sounding at 1800 UTC from KAPG [Fig. 6b] shows that the temperature between the surface and 700 hPa range from -1.3 to 0.5°C (warmed  $\approx 2^\circ\text{C}$  from the 1200 UTC sounding at KAPG), and the wind profile is similar to that observed at 1200 UTC. By 0000 UTC [Fig. 6d] the temperature between the surface and 700 hPa has cooled by as much as  $6^\circ\text{C}$ , and the upper-level winds were primarily out of the north-northwest between the surface and 500 hPa.

Figure 7 depicts three flashes that occurred 8 minutes apart between 21:11:00 UTC and 21:19:00 UTC. The northward advection of the flash locations with time matches the wind direction between 2 and 6 km from the KAPG sounding at 1800 UTC [Fig. 7b]. Each of the flashes initiated along Maryland's eastern shore and then propagated westward across the Chesapeake Bay and into central Maryland.

The first flash during this period occurred at 21:11:12.90 UTC and culminated just south of Baltimore [Fig. 7A]. The flash was  $463\text{ km}^2$  and the NLDN identified three separate IC flashes with this one LMA-derived flash. Zero communications towers were noted at the initiation location of the flash. One of the three flashes was a +IC flash, and the remaining two were -IC flashes. The timing of these flashes were delayed by 200-300 ms when compared to the LMA data. One +IC component was detected at 21:11:13.20 UTC nearly 300 ms after flash initiation. The two -IC flashes at 21:11:13.61 UTC and 21:11:13.64 UTC were recorded nearly 200 ms after the last VHF source point detected by the DCLMA for this flash (and thus do not appear in the time-height plot of Fig. 7A). Importantly, the two -IC events were identified within 70-90 m of

the location of a communications tower at latitude/longitude 39.180, -76.536, after the LMA-flash terminated.

The second flash at 21:14:48.78 UTC was the largest flash of the three with an area encompassing 1938 km<sup>2</sup> [Fig. 7B]. The NLDN identified six +IC components with this single LMA-derived flash in Queen Anne's County, MD. All six +IC flashes were associated with the early development of the LMA flash. Next the leader propagated westward toward Baltimore, over the northern end of Chesapeake Bay, sloping downward from an average height of 5 km down to approximately 2.5 km in height [Fig. 7B, blue and cyan dots]. The NLDN observed a +185 kA CG flash at 21:14:49.08 UTC at latitude/longitude 39.222, -76.652, in far northern Anne Arundel County, MD as the flash skirted the southern end of the city of Baltimore. A tower was not recognizable at the location of the flash initiation, and three VHF source points were observed by the DCLMA around 5 km in altitude prior to the downward extension of two VHF source points to the surface in Fig. 9. Thus, this flash was likely initiated in the cloud and not from the ground. A tower was also not observed at the +CG ground flash location. The flash continued westward into Howard and Montgomery Counties until terminating near Rockville, MD. The NLDN also identified a +IC component (+13.4 kA), approximately 300 ms after the time the LMA identified the leader passed the location of the flash detection.

The final flash in this series occurred at 21:18:46.35 UTC and was the smallest of the three flashes [Fig. 7C]. It was only approximately 85 km<sup>2</sup> in size and initiated once again over Queen Anne's County, Maryland. The leader for this flash then propagated westward over the Chesapeake Bay and terminated over the southern end of Baltimore, Maryland. The NLDN identified one -IC event and one -CG stroke at 21:18:46.04 and 21:18:46.05 UTC, respectively.

The NLDN-identified CG had a magnitude of -13.2 kA. In this case, the NLDN observes the -IC and -CG flashes 300-350 ms before the first VHF source point from the LMA.

### **3.3 24 December, 2009, Central OK**

On 24 December 2009, a blizzard event occurred in Central OK. Upwards of 25 cm of snow fell during the event, and winds gusted as high as  $27 \text{ m s}^{-1}$ . Three lightning flashes occurred at 19:50:00.08 UTC, 19:54:16.50, and 19:58:03.40 UTC in McClain County, OK on 24 December 2009. Two of these flashes are shown in Fig. 8. The three flashes were all found in a transition region between sleet and heavy snow within this winter system [Kuhlman and Manross, 2011]. An 1800 UTC sounding from Norman, OK illustrated the vertical thermodynamic and kinematic environment found near lightning flash occurrence [Fig. 8A]. All three flashes in this event occurred within temperatures between 0 and  $-10^{\circ}\text{C}$  (altitudes less than 4 km in height) in the same general horizontal region [Figs. 8 B,C]. Of the three LMA-identified flashes only one was detected by the NLDN and was designated as an IC event [Fig. 8C, black diamonds]. The inferred charge structure of these flashes was positive over negative charge based on the LMA, sounding, and NLDN information.

The first flash at 19:50:00.08 UTC had two distinct altitudes of propagation, as inferred from the LMA data. One altitude was located below 1 km and a second between 1.5 and 3 km [Fig. 8B]. The VHF sources below 1 km in this flash were real because they were near the center of the LMA network, were still present with a 10 LMA station solution, they were not a reflection of the flash at higher altitudes, and the sounding from this event showed that cloud base heights were as low as 650 m. This flash had an area of  $294 \text{ km}^2$ , with the longest axis of the flash approximately 34 km in length in the north/south direction.

The second flash at 19:54:16.48 UTC initiated approximately 7 km to the northeast of the first and contained a very similar bi-level structure. The majority of VHF sources were found below 1 km or between 1.5 and 4 km [Fig. 8C]. Six IC flashes were detected by the NLDN and was located at the location of a radio station communications tower (34.901, -97.568). The timing of the VHF sources at this location do not coincide with the timing of the NLDN strokes, as there is more than a 300 ms difference between the first VHF points and the first NLDN stroke. Leader speed analysis for this flash [Fig. 8D] illustrates that the leader speeds were indicative of a positive leader from the tower. The area of this flash was only 108 km<sup>2</sup>. The longest axis of the flash was approximately 18 km in length in the north/south direction.

The third and final flash of the event occurred at 19:58:03.48 UTC and is not shown in this work. This flash did not have a notable bi-level structure because most of the VHF sources were located between 1.5 and 3 km like the first two flashes. No readily identifiable tall human-built objects were identified near the first VHF source locations. This was the smallest flash of the three, only reaching 70 km<sup>2</sup>, with the major axis of the flash being 15 km in the north/south direction like the flashes presented in Fig. 8B and 8C. No additional flashes were observed near the snowfall in central OK after the 19:58:03.48 UTC flash.

### **3.4. 6-7 February 2010, Baltimore, MD**

Heavy snowfall fell in Northern Virginia, Washington D.C., and Maryland between 6 and 7 February 2010. Upwards of 50 cm of snow fell during this two day period. Some of the heaviest snowfall to occur during the event was found during the early morning hours on 6 February between Baltimore MD and Washington D.C. Between 0900 and 1000 UTC, lightning was observed between Baltimore MD and Washington D.C. by the DCLMA.

Figure 9 shows a flash detected at 09:40:29.01 UTC by the DCLMA during the 6 February 2010 thundersnow event. This lightning flash encompassed an area of 283 km<sup>2</sup>. The flash appeared to initiate from a communications tower near television affiliate WBAL-TV in Baltimore, MD (39.335, -76.650) because of the location of the 1st VHF source point from the DCLMA and the identification of two small amplitude IC flashes of -7.3 and -4.5 kA at the tower's location at 09:40:29.01 and 09:40:29.02 UTC, respectively. DCLMA VHF source data suggest that there were two main charge layers within the heavy snowfall: a negative charge region was located between 0 and -5°C ( $\approx$ 3 km), while an upper positive charge region was observed between -10 and -16°C ( $\approx$ 5 km) using a sounding from 0900 UTC at KBWI [Fig. 9B,C].

This flash was comprised of three portions [Fig. 9]. Initially, a tower-initiated positive leader propagated along a path approximately 1.5 km in altitude before a negative leader rapidly accelerated upwards to 5 km, and then propagated horizontally once again through the cloud. This occurred two additional times as the lower positive leader propagated southwestward, at approximately 09:40:30.10 and 09:40:30.40 UTC. NLDN information indicated that this flash came to ground at two separate locations along its path. The first location was at latitude/longitude 39.239, -76.737 at 09:40:29.77 UTC. This location had the stroke with the largest peak current (-48.1 kA). The second location of CG activity was at latitude/longitude 39.188, -76.897 at 09:40:30.30 UTC. Here three ground strokes were observed by the NLDN with peak amplitudes of -15.5, -14.9 and -22.2 kA, respectively.

The plausibility of the tower initiating the first flash was reinforced by additional LMA events that were not included in this analysis due to poor low-level coverage by the LMA. Five additional flashes were observed by the DCLMA network between 09:42:00 and 09:57:00 UTC on 6 February 2010 [Fig. 11A]. However, because these flashes occurred on a gradient in the

DCLMA's detection efficiency, much of the low-level coverage of these events was not captured because the flash information was below the DCLMA's line of sight in this area [Fig. 11B, C]. Although these flashes were omitted from this analysis, the NLDN data point to the same tower location as the first flash. A total of 21 NLDN flash detections occur during this period in Maryland. Of the 21 NLDN flash detections, 17 occur within 500 m of the same tower location as the flash analyzed above (14 IC, 3 CG). Additional discussion on the LMA line of sight and the importance of precursor VHF sources is provided in Section 4.1 below.

### 3.6 Overall Characteristics of Electrified Snowfall Lightning Events

A total of 34 flashes are analyzed in this study. Characteristics of each LMA-derive flash are listed in Tables 1 and 2. The areal extent of these flashes and the number of NLDN flash associations have not been reported in the literature, and flash polarity information should complement other studies that have examined the thundersnow phenomenon [e.g., *Market and Becker*, 2009; *Warner et al.*, 2014]. Eleven of the 34 flashes initiated from tall human-made objects like communication towers [e.g., Figs. 1, 3, 5, 9].

The mean area encompassed by this set of flashes is 375 km<sup>2</sup>, with a maximum flash extent of 2300 km<sup>2</sup>, a minimum of 3 km<sup>2</sup>, and a median of 128 km<sup>2</sup>. Two additional LMA flashes had areas greater than 1000 km<sup>2</sup> (1674 km<sup>2</sup> and 1938 km<sup>2</sup>). The 1674 km<sup>2</sup> flash produced the largest peak amplitude negative flash (3 strokes, -125.0 kA), while the 1938 km<sup>2</sup> flash produces the largest peak amplitude positive flash (1 stroke, +185.0 kA). The largest area flash [Fig. 1] had 4 separate NLDN-identified ground flash locations with peak amplitudes of -78.0, -53.0, -35.0 and -10.0 kA, respectively.

The majority of the lightning flashes studied in this small sample contained a normal polarity charge structure, where a positive charge region occurred above a negative charge region

[e.g., Figs. 1, 3, 5, 9]. Large stratified regions of charge were observed in these events. This characteristic is similar to the charge structure observed in stratiform regions of mesoscale convective systems or forward anvils in supercell storms [e.g., *Lang et al.*, 2004; *Carey et al.*, 2005; *Kuhlman et al.*, 2009; *Weiss et al.*, 2012]. In one instance, there was evidence of sloped charge layers, as the lightning propagated through a region with larger vertical growth [e.g., Figs. 3, 4].

One common observation from the case studies was that multiple NLDN-derived flashes can be associated with a single LMA-derived flash. Seventy-eight NLDN-derived flashes were identified with the 34 LMA-derived flashes in this study. As many as 11 NLDN-derived flashes were associated with a single LMA flash [e.g., Fig. 1]. The breakdown of NLDN flashes was as follows: 48 of the NLDN flashes were identified as IC, while 30 of them were identified as CG. The mean ratio of NLDN-identified flashes (IC plus CG) to one LMA derived flash is 2.29, with 7 of the 34 flashes containing zero NLDN detections. Furthermore, 22 of the 34 LMA flashes contained at least one CG flash (65%).

Ground flashes of both polarities were observed in this study. A total of nine positive CG flashes were found in the sample of 34 flashes, with a maximum peak amplitude of +185.0 kA. All 9 positive flashes occurred in the 26-27 January 2011 event near Washington, DC. The mean amplitude of the 9 flashes is +89.0 kA with a median value of +87.0 kA. Twenty-two negative CG flashes were observed in this sample. The largest magnitude negative CG flash was -125.0 kA, and the population's mean and median were -39.0 kA and -17.0 kA, respectively.

## 4. Discussion

### 4.1 Precursor Sources at Tower Locations

In Fig. 9, the authors present a tower-initiated flash which begins at a tall communications tower in Baltimore, MD. The difference between this event and other tower-initiated flashes examined was that there is not a clear VHF source trail from the tower location to the main channel that develops around 2 km at 09:40:29.40 UTC. This behavior was observed for similar LMA observed events on that same day that were not included in the work [Fig. 10A]. Precursor VHF sources have been observed prior to the initiation of lightning in the cloud in previous work [e.g., *Lang et al.*, 2014]; however, the difference between those events and this particular event was that the NLDN also detects lightning at the location of the tower at the same time as the first VHF source.

One plausible explanation for the lack of VHF sources between the tower location and the rest of the lightning flash was the DCLMA's line of sight during the event. Using a source detection efficiency estimation technique by *Chmielewski and Bruning*, [2016], one can observe that the initial part of the flash is located in a gradient region of detection efficiency [Fig. 10B]. The average error in vertical location of these source events was on the order of 100-200 meters at a range of 85 km and a height of 1.0 km. VHF sources were nearly undetectable below ~0.5 km [Fig. 10C]. Figure 10A also shows that there is a cluster of 17 NLDN flash detections at the same communications tower between 09:42:00 and 09:57:00 UTC on 6 February 2010. Given the repeated nature of lightning observed in other snowfall events in the present study and in other publications [e.g., *Warner et al.*, 2014; *Kumjian and Deierling*, 2015], it is very plausible that the initial detection of this flash (and other flashes shown in Fig. 10A) was missed by the DCLMA because of line of sight and position errors due to the range of the flash from the LMA center. This

hypothesis partially explains the different flash detection sequence observed for this flash between the VHF and NLDN information, as compared to other tower-initiated lightning flashes in Figs. 1, 3, and 5.

#### **4.2 Flash Initiation within the Human-Built Environment**

Lightning at the location of tall manmade objects has been documented by several investigators in the last few years [e.g., *Schultz et al.*, 2011; *Warner et al.*, 2014; *Kingfield et al.*, 2017]. Previous work by *Warner et al.*, [2014] showed that the NLDN detected a flash within 50 km and 500 ms prior to upward lightning from a tall object. Figures 1, 3, and 5 show slightly different behavior than previously noted, where the tower is initiating the flash in the absence of an existing lightning flash. In these two flashes the upward leader starts from the tower location, propagates into the cloud, and then a return stroke travels back to the tower location. The delay in this return propagation was 200 ms for the flash in Fig. 1 and 600 ms for the LMA-derived flash in Fig. 5. Thus, it appears that the NLDN data are detecting the return stroke back to the tower and not the initial upward leader when one compares the LMA and NLDN timing of the lightning flash detection. This observation is supported by temporal delays between high speed video of tower-initiated lightning and ground based NLDN-like datasets in *Saba et al.*, [2016]. It is unclear if the presence of IC events at tower locations are the misclassification of CG events [*Biagi et al.*, 2007], or if they are quieter additional upward leaders from the tower that are being masked by noisier positive breakdown [*Rison et al.*, 1999].

Another observation was that the leader speed of the upward propagation of lightning flashes from towers are slower than the leader speeds of naturally occurring upward leaders in the cloud within these cases. An order of magnitude difference in leader speed was observed when directly comparing the upward leader from the tower in 04:31:57 UTC flash on 10 January 2011

with the upward leader within the cloud from this same lightning flash [Fig. 2]. Slower leader speeds were observed for the other tower-initiated flashes presented in this work (not shown).

Finally, there will be instances where the human built object that initiated the flash may not be readily identifiable. The three lightning flashes in the 24 December 2009 event in Central OK have the potential to initiate from the human built environment because of VHF sources below 0.5 km and NLDN locations at a communications tower, and leader speed analysis in Fig. 8D supports the idea of a positive leader from the ground. However, in this specific case it was very difficult to ascertain the exact location of initiation because of the low altitudes of the initial VHF source points and lack of NLDN data in 2 of the 3 flashes.

#### **4.3 GLM and the detection of lightning in heavy snowfall**

One of the main caveats to the present study is the small sample size. The 34 lightning flashes used in this study likely does not represent the full gamut of lightning events observed in nature. The LMA systems used in this study have a combined total of 4 electrified snowfall events out of a possible 36 years of combined operation. Therefore, GLM will be a useful tool to continue assessing lightning in heavy snowfall events given its large field of view and the detection of the spatial extent of lightning. When combined with ground based networks like the NLDN, the potential to extend the observations of flash size, number of ground flash locations, and interactions with tall man-made objects presented in this work. Furthermore, the GLM can provide metrics of flash energy, which is hypothesized to be more directly related to generation of charge within the cloud than flash rate based approximations [Boccippio 2002].

To demonstrate the potential GLM has for furthering the understanding of lightning in heavy snowfall, the authors present an analysis of a lake effect snowfall from the GLM checkout phase in 2017. Figure 11 shows GLM event-level data from the National Oceanic and Atmospheric

Administration's (NOAA) GOES Rebroadcast (GRB) during lake effect snowfall on between 0130 and 0200 UTC on 27 November 2017 in Western New York. A total of four lightning flashes were identified by the GLM lightning cluster filter algorithm [LCFA, *Goodman et al.*, 2012] during this period at 01:37:29, 01:42:31, 01:46:27, and 01:59:55 UTC. GLM flash sizes were on the order of 1 GLM pixel ( $\leq 64 \text{ km}^2$ ) up to 5 GLM pixels ( $\sim 320 \text{ km}^2$ ). The NLDN detected 8 -IC flashes during this 30 minute period. All 8 flashes were observed between 01:59:55.72 and 01:59:55.82 UTC and were closest in space and time to the GLM flash at 01:59:55 UTC in Fig. 11C. All 8 NLDN detections were also located at a television communications tower at latitude/longitude 43.863, -75.727, which is not an uncommon occurrence in Western New York [*Steiger and Kranz*, 2017]. In fact, examining Fig. 11A, B, and C, one can observe that all four of the flashes occur in the same exact location near this tower within the GLM field of view.

Further analysis of the event beyond flash occurrence, gross spatial characteristics, and association with NLDN data is not possible at this time. Navigation and timing of the GLM data are still being worked by NOAA during GLM's checkout phase [Dr. Steven J. Goodman, GOES-16 Chief Scientist, personal communication], and thus in depth analysis is not possible until these the data are standardized within GLM data stream and NOAA's Comprehensive Large Array-data Stewardship System (CLASS) archive for satellite data. The planned release for this information is by June of 2018. The navigation issue is most notable in the spatial offset between the NLDN data and the GLM data. There are also minor temporal offsets that are less than one second in the current data that would affect the interpretation of the timing between the GLM data and the NLDN data. Future work will reexamine these flashes once the satellite navigation and timing are incorporated into the Level 2 GLM data provided from the GRB. However, GLM as Fig. 11 demonstrates, GLM will observe lightning within heavy snowfall events.

## 5. Conclusions

Thirty-four lightning flashes from four electrified snowfall events were examined using LMAs and the NLDN, providing insight into the spatial characteristics of lightning in these winter events. The primary observations demonstrate that lightning detected within electrified snowfall are likely to contain the following characteristics:

- 1) The primary charge structure observed in this sample of 34 LMA derived flashes was positive charge over negative charge.
- 2) Eleven of the 34 LMA derived flashes analyzed were initiated by tall human built objects (e.g., communications towers).
- 3) Multiple NLDN-based flash detections (IC and/or CG) can be associated with a single LMA-derived flash. An average of 2.29 NLDN flashes were associated with one LMA flash, with a maximum of 11 NLDN flashes associated with one LMA flash.
- 4) Seven LMA-derived flashes in this study were not detected by the NLDN.
- 5) The peak positive (negative) amplitude measured in these four case studies is +185 kA (-125.0 kA), the average peak amplitude is +89.0 kA (-39.0 kA) and the median peak amplitude is +87.0 kA (-17.0 kA).
- 6) Evidence of negative dart leaders traveling back to the ground along the upward leader path from the tower initiation was observed in at least six of the eleven tower-initiated flashes. Time delays between the upward leader in the LMA data and the NLDN observing the lightning at a tower location were up to 600 ms after the LMA initially observed the lightning event.
- 7) The average area encompassed by this set of flashes was 375 km<sup>2</sup>, with a maximum flash extent of 2300 km<sup>2</sup>, a minimum of 3 km<sup>2</sup>, and a median of 128 km<sup>2</sup>.

GLM should increase the availability of total lightning observations to the forecasting, modeling, and research community for analysis of electrified snowfall events. GLM provides operational weather forecasters additional lightning characteristics (e.g., flash area, flash radiance), which are important in locating the areas with the most intense snowfall rates, especially in areas where radar coverage is poor (e.g., the Western United States). Further research should also be done to determine if the occurrence of lightning in these events provide additional utility for short-term (<30 minute) resource planning of high impact snowfall events when lightning is present.

#### *Acknowledgements*

C. Schultz and T. Lang would like to thank NASA Science Mission Directorate Science Innovation Funds for funding this work. Lightning mapping array data can be obtained through the Global Hydrology Resource Center (GHRC), which hosts both the DCLMA and the NALMA. The OKLMA data can be obtained through the National Severe Storms Laboratory. The NLDN was purchased via Vaisala, Inc. The XLMA viewing software can be obtained from New Mexico Tech. The authors would also like to recognize Dr. Kyle Wiens for providing the ANGEL software package that was used to overlay LMA data with radar data.

The authors would like to recognize Mr. Jeff Bailey, Dr. Don MacGorman, and Dr. Scott Rudlosky for continual support and maintenance of the North Alabama, Oklahoma, and Washington D.C. LMA sensor networks. Sounding information is available from the University of Wyoming or the University of Alabama-Huntsville. ARMOR radar data are available from the University of Alabama-Huntsville. The authors gratefully acknowledge Dr. Lawrence Carey and Dr. Kevin Knupp for the use of the ARMOR data in Fig. 5. The authors thank Dr. Steven J. Goodman and Dr. Geoffrey Stano for assistance with the GLM data highlighted in this study. GLM data will be available within the NOAA CLASS system in 2018. Finally, the authors would like

615 to thank constructive reviews from 3 anonymous reviewers that improved the content and structure  
616 of this article.

617

## REFERENCES

- Bech, J., N. Pineda, T. Rigo, and M. Aran (2013), Remote sensing analysis of Mediterranean thundersnow and low-altitude heavy snowfall event, *Atmos. Res.*, **123**, 305-322.
- Benjamin, S. and Coauthors (2004), An hourly assimilation-forecast cycle: the RUC. *Mon. Wea. Rev.*, **132**, 495-518.
- Biagi, C. J., K. L. Cummins, K. E. Kehoe, and E. P. Krider (2007), National Lightning Detection Network (NLDN) performance in southern Arizona, Texas and Oklahoma in 2003-2004, *J. Geophys. Res.*, **112**, doi:10.1029/2006JD007341.
- Bitzer, P. M., J. C. Burchfield, and H. J. Christian (2016), A Bayesian approach to assess the performance of lightning detection systems, *J. Atmos. and Oceanic Tech.*, **33**, 563-578.
- Boccippio, D. J. (2002), Lightning scaling relationships revisited, *J. Atmos. Sci.*, **59**, 1086-1104.
- Bruning, E. C., and R. J. Thomas (2015), Lightning channel length and flash energy determined from moments of the flash area distribution, *J. Geophys. Res. Atmos.*, **120**, 8925–8940, doi:10.1002/2015JD023766.
- Bruning, E. C. and D. M. MacGorman (2013), Theory and observations of controls on lightning flash spectra. *J. Atmos. Sci.*, **70**, 4012-4029.
- Bruning, E. C., S. A. Weiss, K. M. Calhoun (2014), Continuous variability in thunderstorm primary electrification and an evaluation of inverted-polarity terminology, *Atmos. Res.*, **135–136**, 274-284, doi:https://doi.org/10.1016/j.atmosres.2012.10.009.
- Brook, M., M. Nakano, P. Krehbiel, T. Takeuti (1982), The electrical structure of the Hokuriku winter thunderstorms, *J. Geophys. Res.*, **87**, 1207-1215.
- Buck, T., A. Nag, M. J. Murphy (2014), Improved cloud-to-ground and intracloud lightning detection with the LS7002 Advanced Total lightning sensor, *TECO-2014—WMO Tech. Conf.*

on Meteorological and Environmental Instruments and Methods of Observation, St.

Petersburg, Russia, World Meteorological Organization, **P1(9)**. [Available at:

[https://www.wmo.int/pages/prog/www/IMOP/publications/IOM-116\\_TECO-](https://www.wmo.int/pages/prog/www/IMOP/publications/IOM-116_TECO-)

[2014/Session%201/P1\\_9\\_Buck\\_TotalLightningSensor.pdf](https://www.wmo.int/pages/prog/www/IMOP/publications/IOM-116_TECO-2014/Session%201/P1_9_Buck_TotalLightningSensor.pdf) ]

Campos, L. Z. S., M. M. F. Saba, T. A. Warner, O. Pinto Jr., P. Krider and R. E. Orville (2014),

High-speed video observations of natural cloud-to-ground lightning leaders – A statistical analysis, *Atmos. Res.*, 285-305.

Carey, L. D., M. J. Murphy, T. L. McCormick, and N. W. Demetriades (2005), Lightning

location relative to storm structure in a leading-line trailing stratiform mesoscale convective system, *J. Geophys. Res.*, **110**, doi:10.1029/2003JD004371.

Chmielewski, V. C., and E. C. Bruning (2016), Lightning Mapping Array flash detection

performance with variable receiver thresholds, *J. Geophys. Res. Atmos.*, **121**, 8600–8614, doi:10.1002/2016JD025159.

Crowe, C., P. Market, B. Pettegrew, C. Melick, and J. Podzimek (2006), An investigation of

thundersnow and deep snow accumulations, *Geophys. Res. Lett.*, **33**, doi:10.1029/2006GL028214.

Cummins, K. L. and M. J. Murphy (2009), An overview of lightning location systems: History,

techniques, and data uses with an in-depth look at the U.S. NLDN, IEEE, *Trans. Electromagn. Compat.*, **51**, 499-518.

Dolif Neto, G. and Coauthors, (2009), A comparison of two cases of low-latitude thundersnow,

*Atmosfera*, **22**, 315-330.

Emersic, C., and C. P. R. Saunders (2010), Further laboratory investigations into the relative

diffusional growth rate theory of thunderstorm electrification, *Atmos. Res.*, **98**, 327-340.

Fleenor, S. A., C. J. Biagi, K. L. Cummins, E. P. Krider and X. M. Shao, (2009), Characteristics of cloud-to-ground lightning in warm-season thunderstorms in the Great Central Plains, *Atmos. Res.*, **91**, 333-352, doi:10.1016/j.atmosres.2008.08.011.

Fuchs, B. R., E. C. Bruning, S. A. Rutledge, L. D. Carey, P. R. Krehbiel, and W. Rison (2016), Climatological analyses of LMA data with an open-source lightning flash-clustering algorithm, *J. Geophys. Res. Atmos.*, **121**, 8625–8648, doi:10.1002/2015JD024663.

Goodman, S. J., and Coauthors (2013), The GOES-R Geostationary Lightning Mapper (GLM), *Atmos. Res.*, **125-126**, 34-49.

Goodman, S. J., D. Mach, W. Koshak, and R. Blakeslee (2012), GLM Cluster-Filter Algorithm, NOAA-NESDIS Algorithm Theoretical Basis Document, available online at: <https://www.star.nesdis.noaa.gov/goesr/docs/ATBD/LCFA.pdf>

Kingfield, D. M., K. M. Calhoun, and K. M. de Beurs (2017), Antenna structures and cloud-to-ground lightning location: 1995–2015, *Geophys. Res. Lett.*, **44**, doi:10.1002/2017GL073449.

Kitagawa, N. and K. Michimoto (1994), Meteorological and electrical aspects of winter thunderclouds, *J. Geophys. Res.*, **99**, 10713-10721.

Koshak, W. J., and Coauthors, (2004), North Alabama Lightning Mapping Array (LMA): VHF source retrieval algorithm and error analysis, *J. Atmos. Ocean. Tech.*, **21**, 543-558.

Krehbiel, P. R., R. J. Thomas, W. Rison, T. Hamlin, J. Harlin and M. Davis (2000), GPS based mapping system retrieval of lightning inside storms, *EOS*, **81**, 21-25.

Krehbiel, P. R. (2008), The DC Lightning Mapping Array, Preprints, 3rd Conf. on Meteorological Applications of Lightning Data , New Orleans, LA, *Amer. Meteor. Soc.*, 3.2.

688 Kuhlman, K. M. and K. Manross (2011), Lightning and polarimetric signatures of two electrified  
689 winter storms in central Oklahoma. *Fifth Conference on Meteorological Applications of*  
690 *Lightning Data*. American Meteorological Society, Seattle, WA, USA, p. 7.4.

691 Kuhlman, K. M., D. R. MacGorman, M. I. Biggerstaff, and P. R. Krehbiel (2009), Lightning  
692 initiation in the anvils of two supercell storms, *Geophys. Res. Lett.*, **36**,  
693 doi:10.1029/2008GL036650.

694 Kumjian, M. R., and W. Deierling (2015), Analysis of thundersnow storms over Northern  
695 Colorado. *Wea. and Forecasting*, **30**, 1469-1490.

696 Lang, T. J. and S. A. Rutledge (2004), The origin of positive cloud to ground lightning flashes in  
697 the stratiform region of a mesoscale convective system, *Geophys. Res. Lett.*, **31**, doi:  
698 10.1029/2004GL019823.

699 Lang, T. J., S. A. Rutledge, B. Dolan, P. Krehbiel, W. Rison, and D. T. Lindsey (2014),  
700 Lightning in wildfire smoke plumes observed in Colorado during Summer 2012, *Mon. Wea.*  
701 *Rev.*, **142**, 489-507.

702 Lang, T. J., J. Li, W. A. Lyons, S. A. Cummer, S. A. Rutledge, and D. R. MacGorman (2011),  
703 Transient luminous events above two mesoscale convective systems: Charge moment  
704 change analysis, *J. Geophys. Res.*, 116, A10306, doi:10.1029/2011JA016758.

705 Nag, A., M. J. Murphy, W. Schulz, and K. L. Cummins (2015), Lightning locating systems:  
706 Insights on characteristics and validation techniques, *Earth and Space Science*, **2**, 65–93,  
707 doi:10.1002/2014EA000051.

708 MacGorman, D. R., and Coauthors (2008), TELEX: The Thunderstorm Electrification and  
709 Lightning Experiment, *Bull. Amer. Meteor. Soc.*, **89**, 997-1013.

710 Market, P. S. and A. E. Becker (2009), A study of lightning flashes attending periods of banded  
711 snowfall. *Geophys. Res. Lett.*, **36**, doi:10.1029/2008GL036317.

712 Market, P. S., C. E. Halcomb, and R. L. Ebert (2002), Thundersnow events over the Contiguous  
713 United States, *Wea. and Forecasting*, **17**, 1290-1295.

714 Market, P. S. and Coauthors (2006), Proximity Soundings of thundersnow in the Central United  
715 States, *J. Geophys. Res.*, **111**, doi:10.1029/2006JD007061.

716 Mecikalski, R. M., Bain, A. L., and L. D. Carey (2015), Radar and lightning observations of  
717 deepmoist convection across northern Alabama during DC3: 21 May 2012, *Mon. Wea.*  
718 *Rev.*, 143, 2,774–2,794, doi: <https://doi.org/10.1175/MWR-D-14-00250.1>

719 Michimoto, K. (1993), A study of radar echoes and their relation to lightning discharge of  
720 thunderclouds in the Hokuriku District, I, Observation and analysis of single flash  
721 thunderclouds in mid-winter, *J. Meteorol. Soc. Jpn.*, **71**, 195-204.

722 Montanyà, J., O. van der Velde, and E. R. Williams (2015), The start of lightning: Evidence of  
723 bidirectional lightning initiation, *Nature-Scientific Reports*, 1-6, doi: 10.1038/srep15180.

724 Montanyà, J., O. van der Velde, and E. R. Williams (2014), Lightning discharges produced by  
725 wind turbines, *J. Geophys. Res. Atmos.*, **119**, doi:10.1002/2013JD020225.

726 Orville, R. E. (2008), Development of the National Lightning Detection Network, *Bull. Amer.*  
727 *Met. Soc.*, **9**, 180-190.

728 Pettegrew, B. P., P. S. Market, R. A. Wolf, R. L. Holle, N. W. Demetriades (2009), A case study  
729 of severe winter convection in the Midwest, *Wea. and Forecasting*, 24, 121-139.

730 Rison, W., R. J. Thomas, P. R. Krehbiel, T. Hamlin and J. Harlin (1999), A GPS-based three  
731 dimensional lightning mapping system: Initial observations in central New Mexico,  
732 *Geophys. Res. Lett.*, **26**, 3573-3576.

733 Rust, W. D., and R. J. Trapp (2002), Initial balloon soundings of the electric field in winter  
 734 nimbostratus clouds in the USA. *Geophys. Res. Lett.*, **29**, doi:10.1029/2002GL015278.  
 735 Saba, M. M. F., C. Schumann, T. A. Warner, M. A. S. Ferro, A. R. de Paiva, J. Helsdon Jr, and  
 736 R. E. Orville (2016), Upward lightning flashes characteristics from high-speed videos, *J.*  
 737 *Geophys. Res. Atmos.*, **121**, 8493–8505, doi:10.1002/2016JD025137.  
 738 Saunders, C. P. R. and H. Bax-Norman and C. Emersic and E. E. Avila and N. E.  
 739 Castellano (2006), Laboratory studies of the effect of cloud conditions on graupel/crystal  
 740 charge transfer in thunderstorm electrification, *Quart. J. Roy. Met. Soc.*, **132**, 2653-2673.  
 741 Schultz, C. J., Bruning, E. C., Carey, L. D., Petersen, W. A. and S. Heckman (2011), Total  
 742 lightning within electrified snowfall using LMA, NLDN, and WTLN measurements. *Eos*  
 743 *Trans. AGU, Fall Meet. Suppl.*  
 744 Schultz, C.J., and Coauthors, (2012), Dual-Polarization Tornadic Debris Signatures Part I:  
 745 Examples and Utility in an Operational Setting, *Electronic J. Operational Meteor.*, **13** (9),  
 746 120–137.  
 747 Schultz, D. M. and R. J. Vavrik (2009), An overview of thundersnow, *Weather*, **64**, 274-277.  
 748 Schultz, D. M. (1999), Lake-effect snowstorms in Northern Utah and Western New York with  
 749 and without lightning, *Wea. and Forecasting*, **24**, 121-139.  
 750 Steiger, S. M. and T. Krans (2017), Lake-Effect Lightning Modification by a Wind Farm, *Eight*  
 751 *Conference on the Meteorological Applications of Lightning Data*, Amer. Meteor. Soc.,  
 752 Seattle, WA.  
 753 Steiger, S. M., R. Hamilton, J. Keeler and R. E. Orville (2009), Lake effect thundersnow  
 754 in the lower Great Lakes, *J. Appl. Meteor.*, **48**, 889-902.

Takeuti, T., M. Nakano, M. Brook, D. J. Raymond and P. Krehbiel (1978), The anomalous winter thunderstorms of the Hokuriku coast, *J. Geophys. Res.*, **83**, 2385-2394.

Thomas, R. P., P. R. Krehbiel, W. Rison, S. Hunyady, W. Winn, T. Hamlin, and J. Harlin (2004), Accuracy of the lightning mapping array, *J. Geophys. Res.*, **109**, doi:10.1029/2004JD004549.

Thompson, E. J., S. A. Rutledge, B. Dolan, V. Chandrasekar and B. L. Cheong (2014), A dual-polarization radar hydrometeor classification algorithm for winter precipitation, *J. Atmos. and Oceanic Technol.*, **31**, 1457-1481, doi: 10.1175/JTECH-D-13-00119.1

Trapp, R. J., D. M. Schultz, A. V. Ryzhkov and R. L. Holle (2001), Multiscale structure and evolution of an Oklahoma winter precipitation event, *Wea. and Forecasting*, **129**, 486-501.

Warner, T. A., T. J. Lang, and W. A. Lyons (2014), Synoptic scale outbreak of self-initiated upward lightning (SIUL) from tall structures during the central U.S. blizzard of 1–2 February 2011, *J. Geophys. Res. Atmos.*, **119**, 9530–9548, doi:10.1002/2014JD021691.

Weiss, S. A., D. R. MacGorman, and K. M. Calhoun (2012), Lightning in the Anvils of Supercell Thunderstorms, *Mon. Wea. Rev.*, **140**, 2064–2079. doi: <http://dx.doi.org/10.1175/MWR-D-11-00312.1>

778

779

780 Table 1. A list of LMA flash time, areal extent, number of NLDN flashes, flash type, polarity,  
 781 and peak multiplicity for the 34 flashes examined.

782 A \* symbol indicates a flash that initiates from a tower.

Event	Time (UTC)	Flash Size (km <sup>2</sup> )	NLDN Flashes	IC	CG	-CG	+CG	Peak Multiplicity
24 December 2009	19:50:00*	294	0	0	0	0	0	0
	19:54:16*	108	6	6	0	0	0	0
	19:58:03*	70	0	0	0	0	0	0
6 February 2010	09:40:29*	282	4	2	2	2	0	3
10 January 2011	04:31:26*	2300	11	7	4	4	0	6
	04:58:30*	890	0	0	0	0	0	0
	05:10:25*	184	1	0	1	1	0	1
	05:24:01*	280	1	0	1	1	0	2
	05:38:25*	102	3	2	1	1	0	1
	05:43:03*	44	2	2	0	0	0	0
26 January 2011	19:15:04	25	3	2	1	1	0	2
	19:18:34	97	2	1	1	1	0	2
	19:27:26	145	3	1	2	1	1	2
	19:34:12	195	0	0	0	0	0	0
	19:39:24	1674	2	0	2	2	0	3
	19:52:55	39	4	3	1	1	0	2
	19:56:44*	109	0	0	0	0	0	0
	19:57:26	108	1	0	1	0	1	1
	20:04:19*	588	1	0	1	0	1	1
	20:11:49	3.3	1	1	0	0	0	1
	20:29:09	221	1	0	1	0	1	1
	20:30:42	110	1	0	1	0	1	1
	20:34:15	349	6	4	2	1	1	1
	20:48:10	569	3	1	2	0	2	2
	20:54:11	711	6	5	1	1	0	2
	21:11:12	463	3	3	0	0	0	0
	21:14:48	1938	7	6	1	0	1	1
	21:18:46	85	2	1	1	1	0	1
	21:52:37	89	1	0	1	1	0	1
	22:01:11	38	0	0	0	0	0	0
	22:05:30*	528	1	0	1	1	0	3
	23:57:10	31	1	1	0	0	0	1
27 January 2011	00:36:55	8	0	0	0	0	0	0
	01:20:57*	60	1	0	1	1	0	1
		12737.3	78	48	30	21	9	42
Statistics	Average	375	2.29	1.41	0.88	0.62	0.26	1.24
	Maximum	2300	11	7	4	4	2	6
	Minimum	3.3	0	0	0	0	0	0
	Median	127.5	1	0.5	1	0	0	1
	Standard Deviation	554	2.48	2.02	0.88	0.85	0.51	1.26

Table 2 – CG flash peak amplitudes and multiplicity of the 22 flashes that contained at least one CG flash. The 24 December 2009 event had zero CG flashes.

Date	Time (UTC)	Peak Amplitude (kA)	Multiplicity
6 February 2010	09:40:29	-48	1
	09:40:29	-16	3
10 January 2011	04:31:26	-10	6
	04:31:26	-52	6
	04:31:26	-79	2
	04:31:26	-21	1
	05:10:25	-14	1
	05:24:01	-21	1
	05:38:25	-5	1
26 January 2011	19:15:04	-90	2
	19:18:34	-32	2
	19:27:26	-25	2
	19:27:26	22	1
	19:39:24	-125	3
	19:39:24	-21	1
	19:52:55	-48	2
	19:57:26	28	1
	20:04:19	35	1
	20:29:09	134	1
	20:30:42	103	1
	20:34:15	137	1
	20:34:15	-10	3
	20:48:10	71.5	2
	20:48:10	27	1
	20:54:11	-13	2
	21:14:48	185	1
	21:18:46	-13	1
	21:52:37	-10	1
	22:05:30	-17	3
27 January 2011	01:20:57	-14	1

790

791

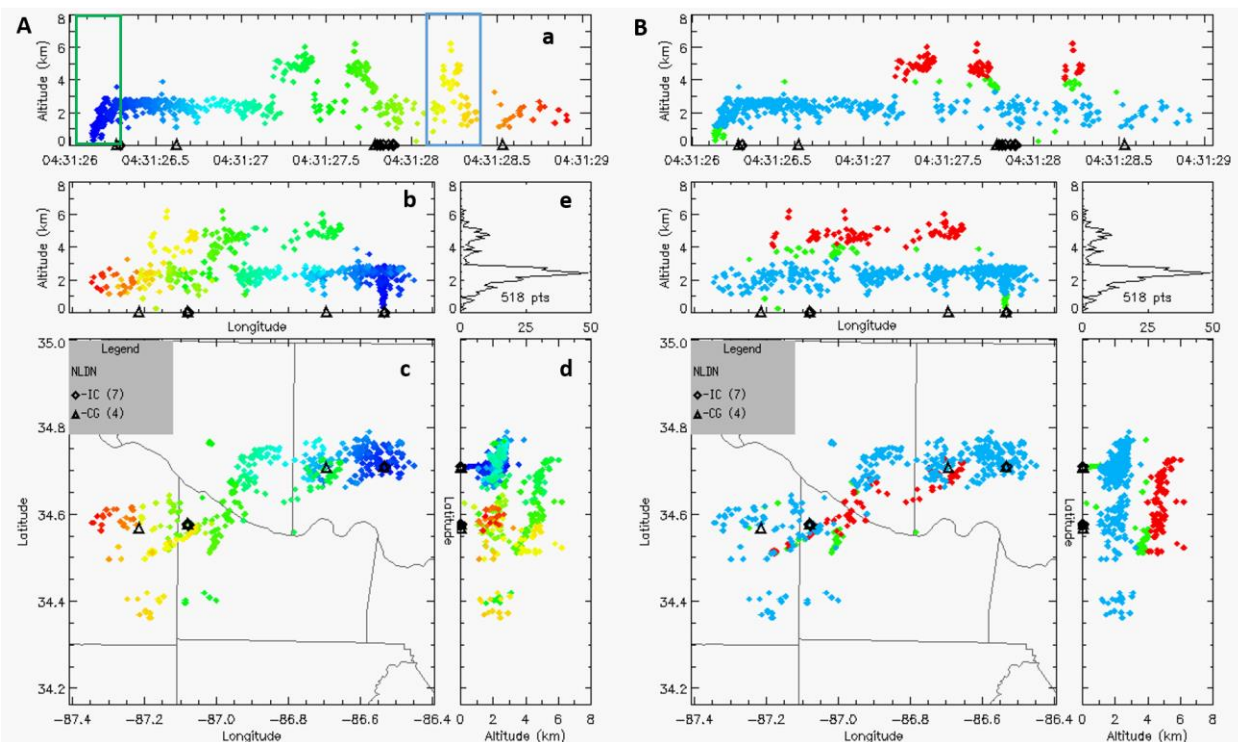


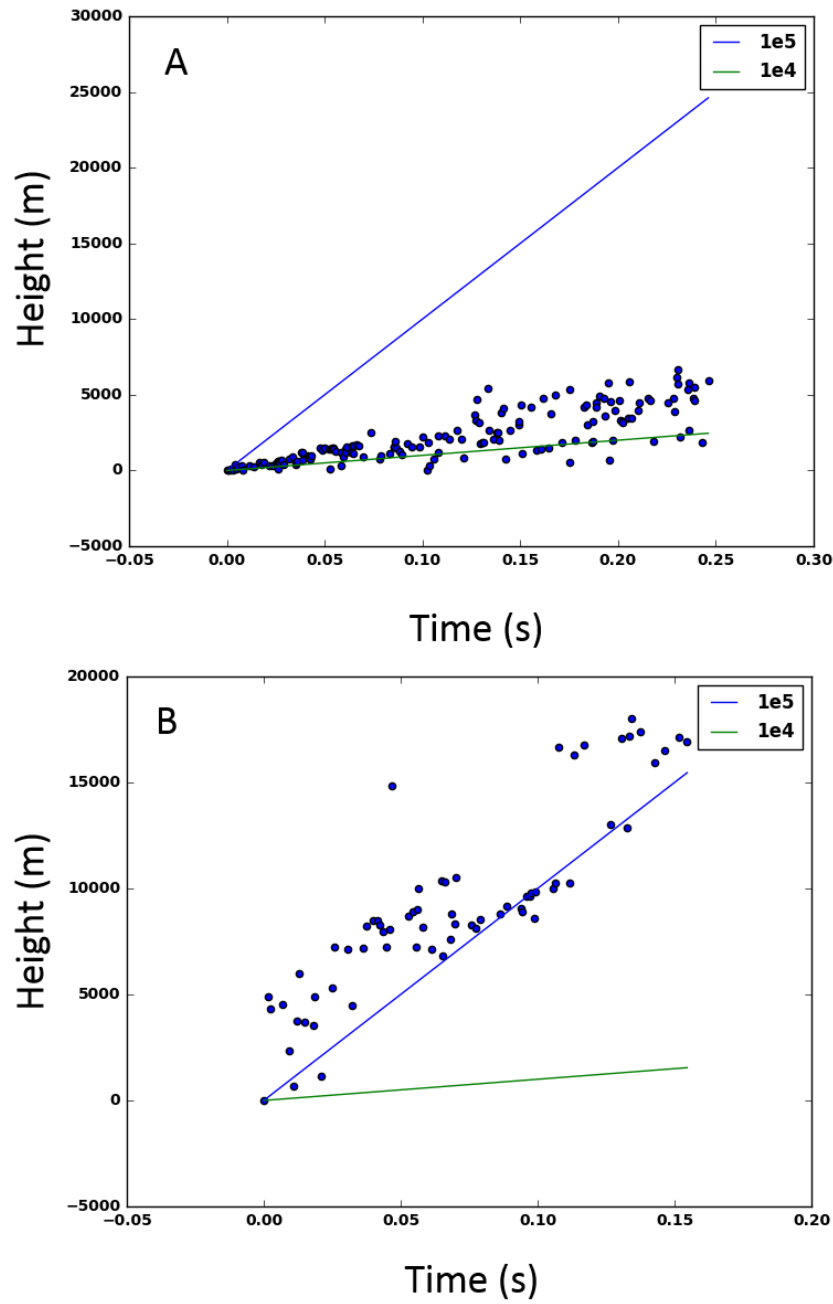
Figure 1A. - An LMA flash at 04:31:26.10 UTC on 10 January 2011 near Huntsville, Alabama using the NALMA. VHF sources from the LMA are represented by the colored dots and the plot is centered relative to the NALMA center. Panel a shows the VHF source information in time and height, Panel b is looking at VHF source information in the longitude direction with height (X-Z plane), Panel c is the VHF source information in plan view in latitude and longitude (X-Y plane), Panel d is the VHF sources information in the longitude direction with height (Y-Z plane), and Panel e is a histogram of the number of sources with height. Labels on the longitude (X) and latitude (Y) axes in Panel C translate to Panels B and D, respectively. Black diamonds represent the location of -IC flashes and black triangles represent the location of individual -CG flash locations as observed by the NLDN. The green box in Panel a indicates the positive leader examined in Fig. 2, and the blue box is the negative leader examined in Fig. 2.

804 Figure 1B - Charge structure analysis derived from the LMA for the same flash. Red dots indicate  
805 the location of positive charge, blue dots are the location of negative charge, and green dots show  
806 the locations of leaders. The NLDN data are represented in the same manner as Fig. 1A.

807

808

809



810

811 Figure 2. Leader speed analysis for the lightning flash at 04:31:26.10 UTC. Panel A corresponds to  
 812 the initial upward leader from the tower in Fig. 1A.a (green box), while Panel B represents the negative  
 813 leader speed that corresponds to the final upward leader in the cloud in Fig. 1A.a (blue box).

814

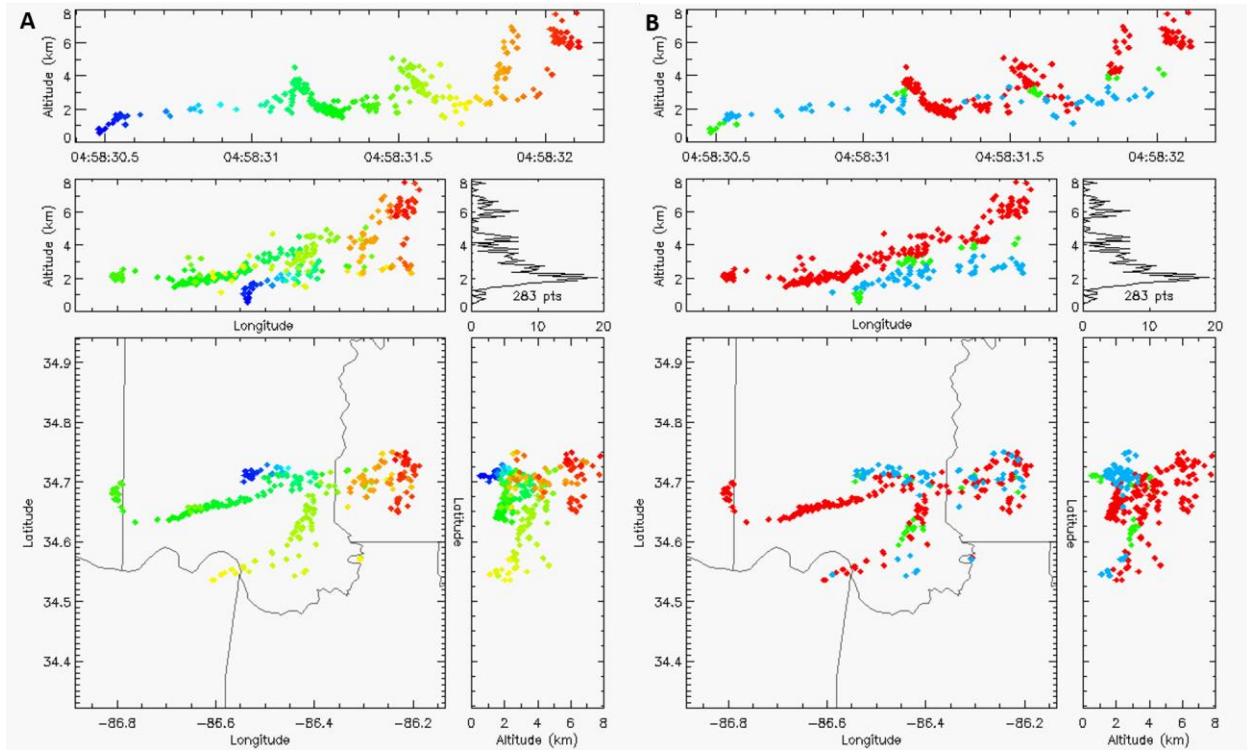


Figure 3. Same as Fig. 1, but for a flash at 04:58:30.48 UTC on 10 January 2011 near Huntsville, Alabama using the NALMA. Zero NLDN observed flashes are found with this flash.

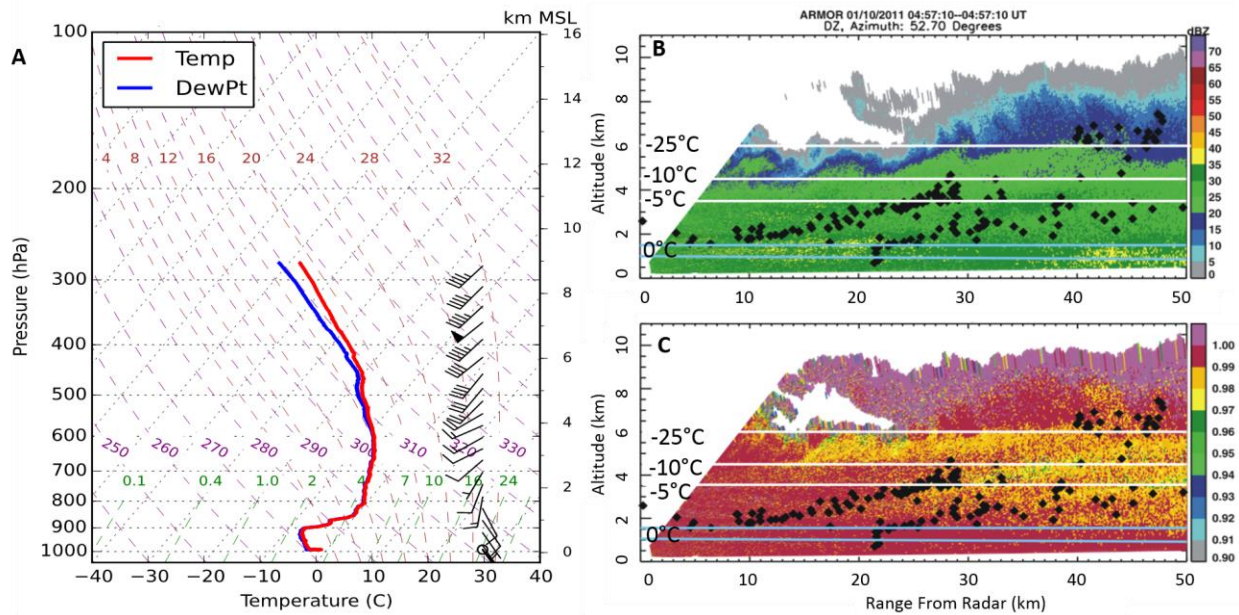


Figure 4. Panel A is an upper-air sounding from the University of Alabama in Huntsville (KUAH) at 0303 UTC on 10 January 2011. Plotted are temperature (red line, °C), dew point (blue line, °C), and wind profile (knots). Panel B is a range-height-indicator (RHI) of radar reflectivity from the ARMOR C-Band polarimetric radar along the 52.7° degree radial at 04:57:10 UTC on 10 January 2011. Panel C is an RHI along the same radial, but for correlation coefficient. The 04:58:30.48 UTC LMA flash (black diamonds) and temperature heights (white/light blue lines) are overlaid on the image and are derived from Fig. 4. White lines reference subfreezing temperatures, while blue lines bookend a layer of the atmosphere where the temperature was at or above 0°C.

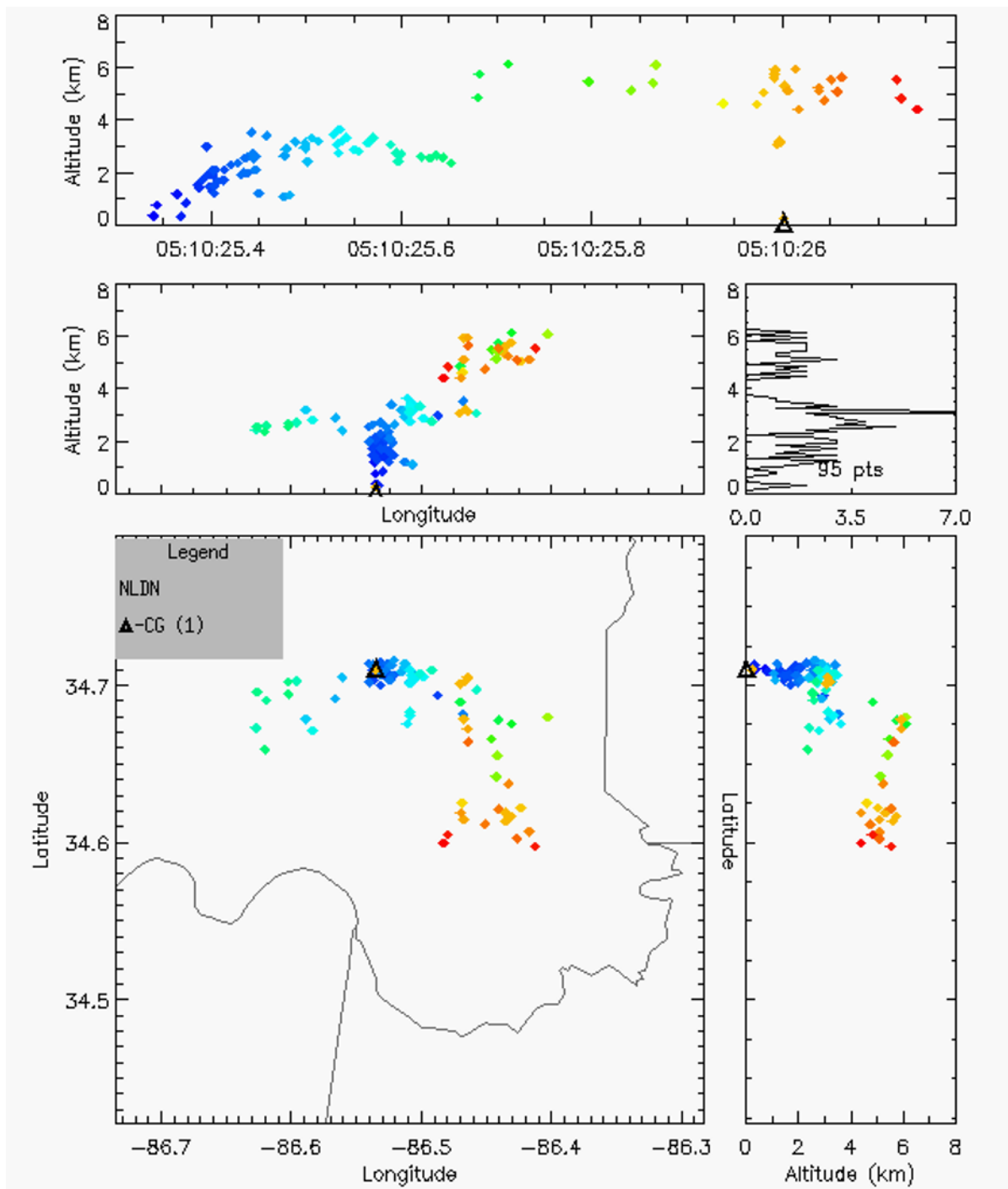
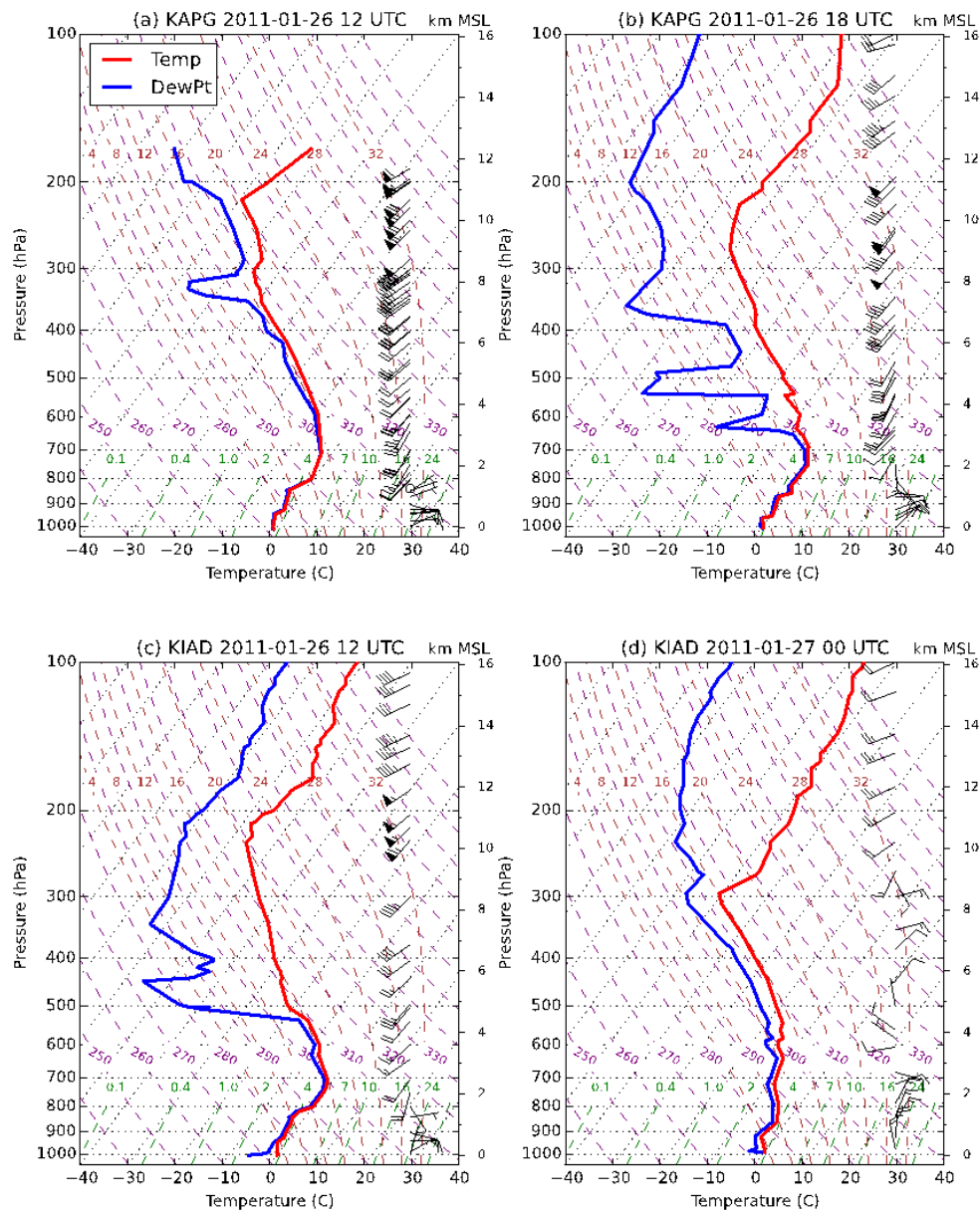


Figure 5. Same as Fig. 1 but for a flash at 05:10:25.34 UTC on 10 January 2011 near Huntsville, Alabama using the NALMA.



836

837 Figure 6. Upper-air soundings at 12 UTC and 18 UTC on 26 January 2011 from Aberdeen Proving  
 838 Ground, Maryland (KAPG; top two panels, a, b) and at 12 UTC on 26 January 2011 and 00 UTC  
 839 27 January 2011 at Sterling, Virginia (KIAD; bottom two panels, c, d) during the 26-27 January  
 840 2011 electrified snowfall event in the Mid-Atlantic Region. Plotted are temperature (red line, °C),  
 841 dew point (blue line, °C), and the wind profile (knots).

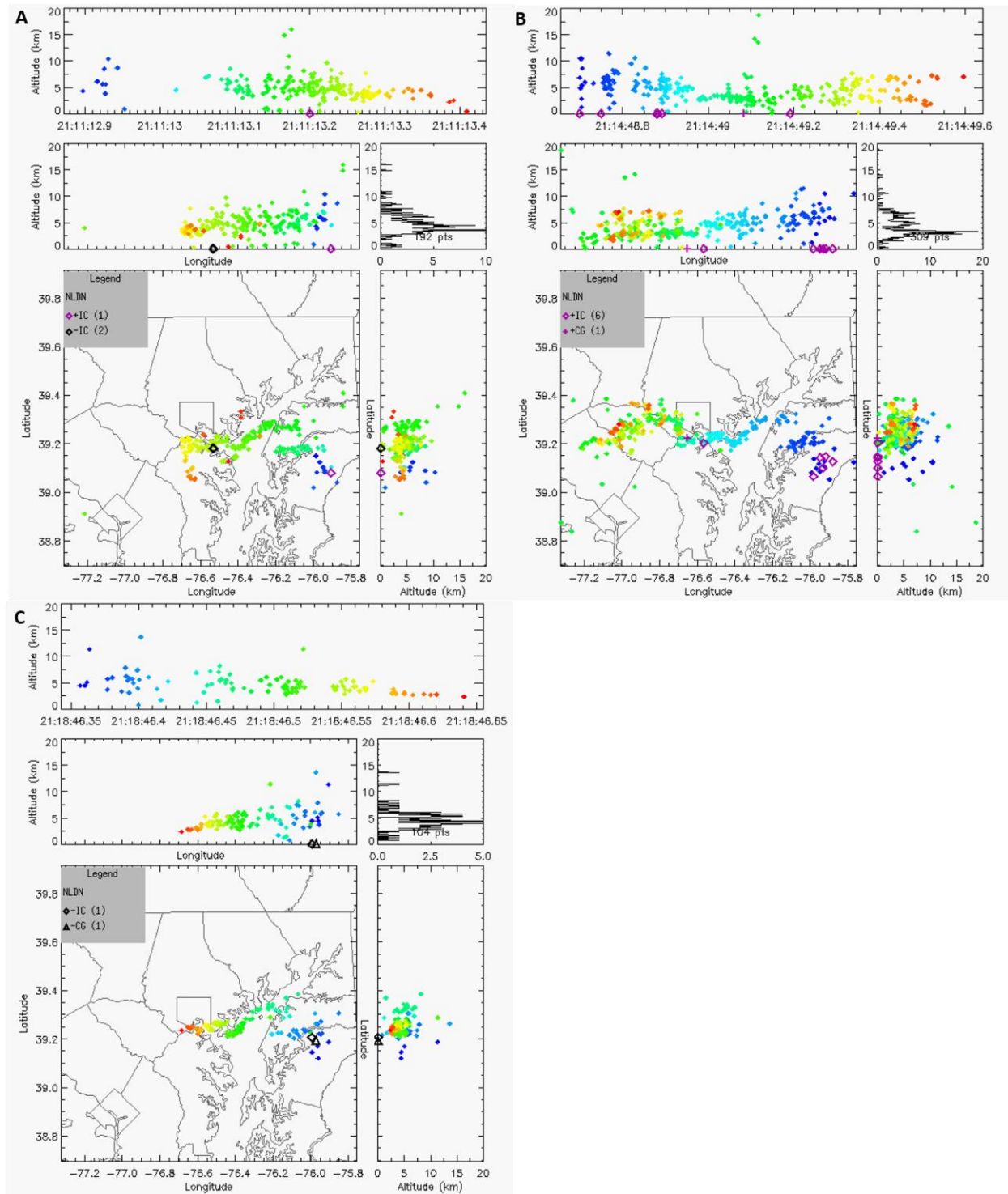


Figure 7. Same as Fig. 1, but for the first in a series of three flashes between 21:11:12.90 UTC and 21:18:46.35 UTC on 26 January 2011 near Baltimore, Maryland as viewed from the DCLMA. Panel A represents a flash occurs at 21:11:12.90 UTC, Panel B is a flash which occurs at

21:14:48.78 UTC, and Panel C is a flash that occurs at 21:18:46.35 UTC. Black diamonds and triangles are the same as in Fig. 1. The purple plus sign is the location of a positive CG flash, and the purple diamonds represent the location of +IC flash detections by the NLDN.

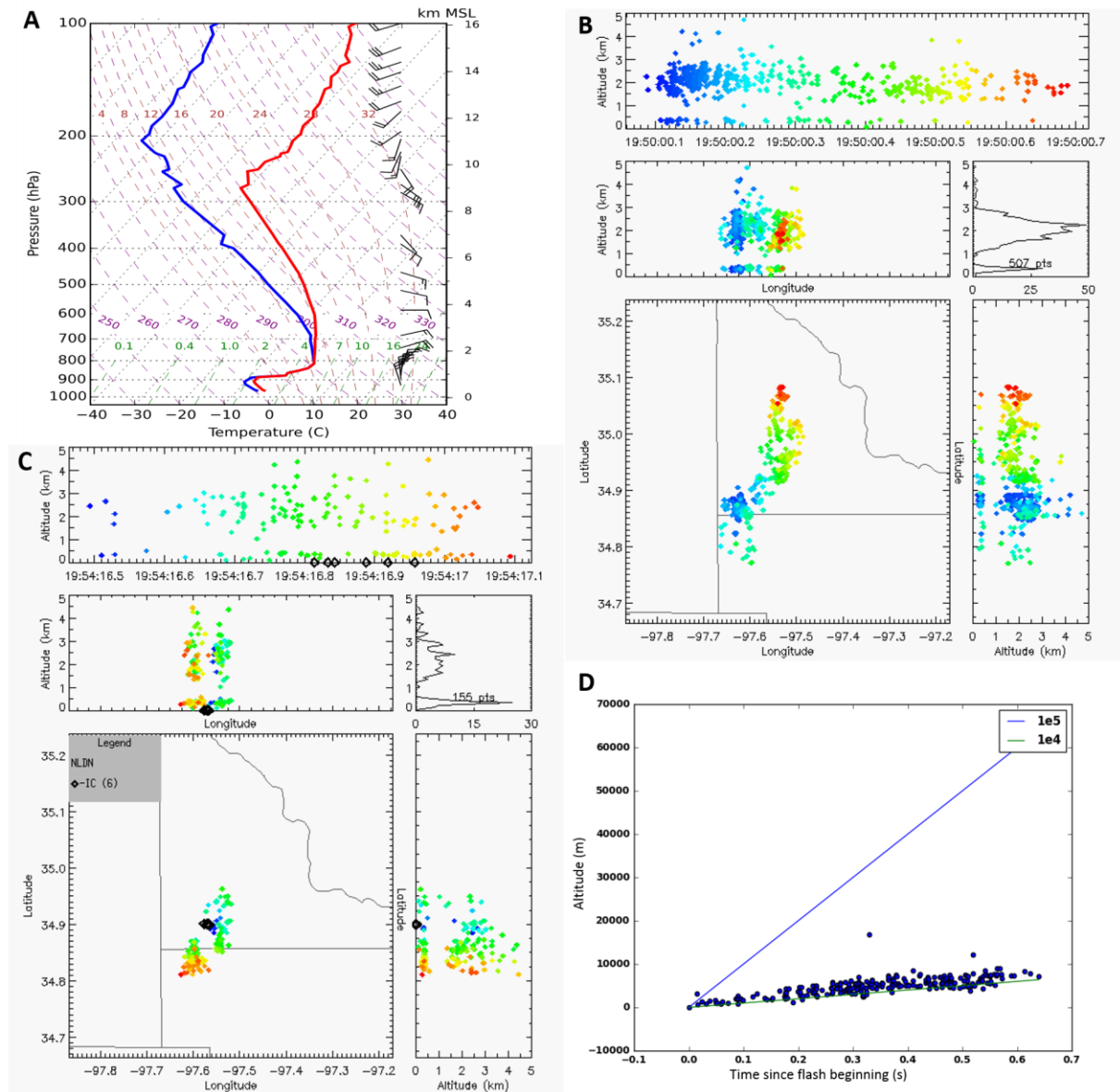


Figure 8. Presented here are upper-air, LMA, and leader speed information for an electrified snowfall event on 24 December 2009 in Central Oklahoma. Panel A is an 1800 UTC upper-air sounding from Norman, Oklahoma (KOUN) on 24 December 2009. Plotted are temperature (red line, °C), dew point (blue line, °C) and wind profile (knots). Panels B and C are the same as Figure 1, but correspond to flashes at 19:50:00:08 UTC and 19:54:16.48 UTC, respectively. Panel D is leader speed information presented the same as in Fig. 2, but for the 19:54:16.48 UTC flash in Panel C.

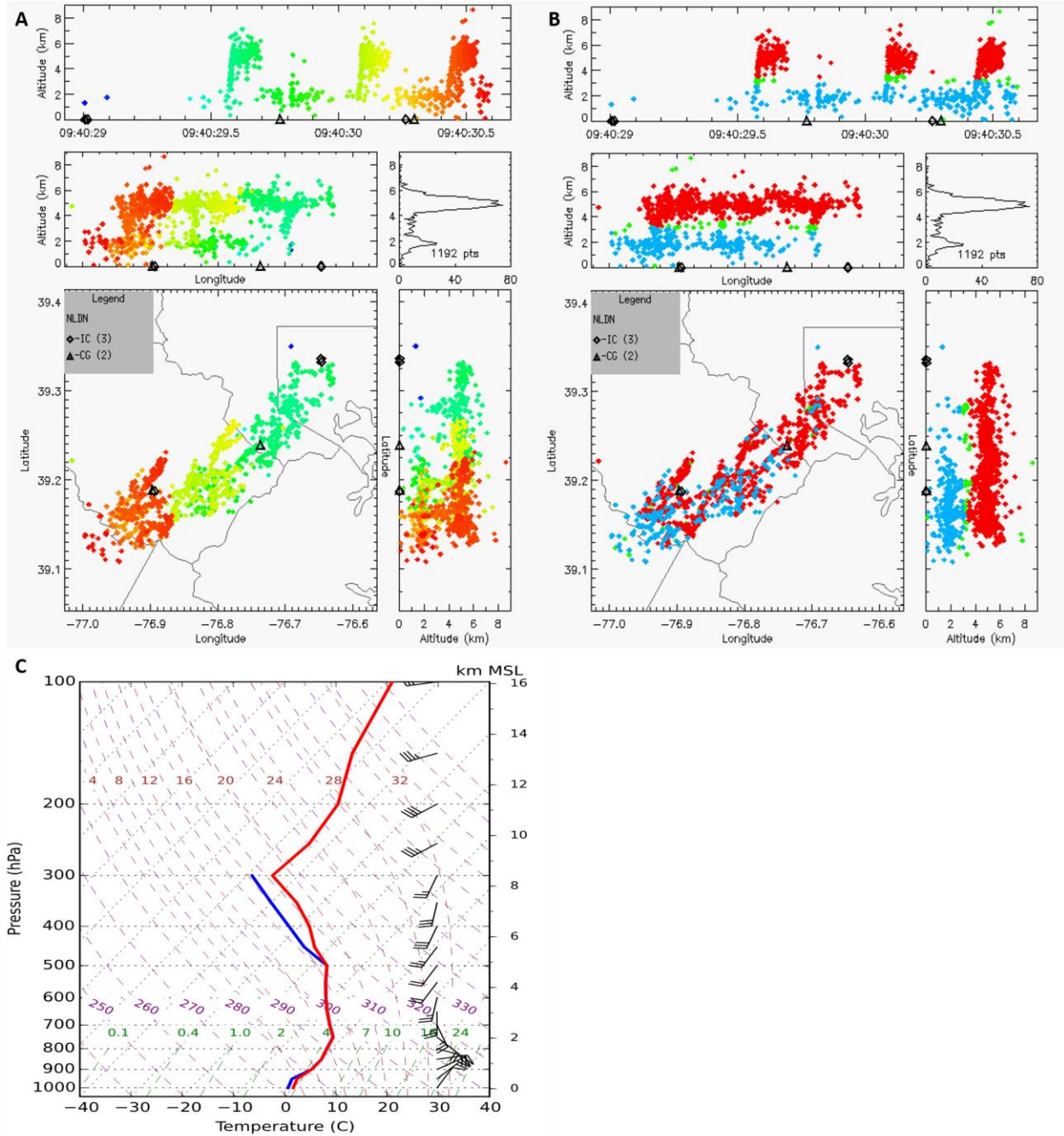


Figure 9. Panels A and B are the same as Fig. 1, but for a flash on 6 February 2010 near Baltimore, Maryland using the DCLMA. Panel C is a zero hour model sounding from the 0900 UTC run of the Rapid Update Cycle model on 6 February 2010 at Baltimore International Airport (KBWI) in Baltimore, Maryland. Plotted are temperature (red line, °C), dew point (blue line, °C) and wind profile (knots).

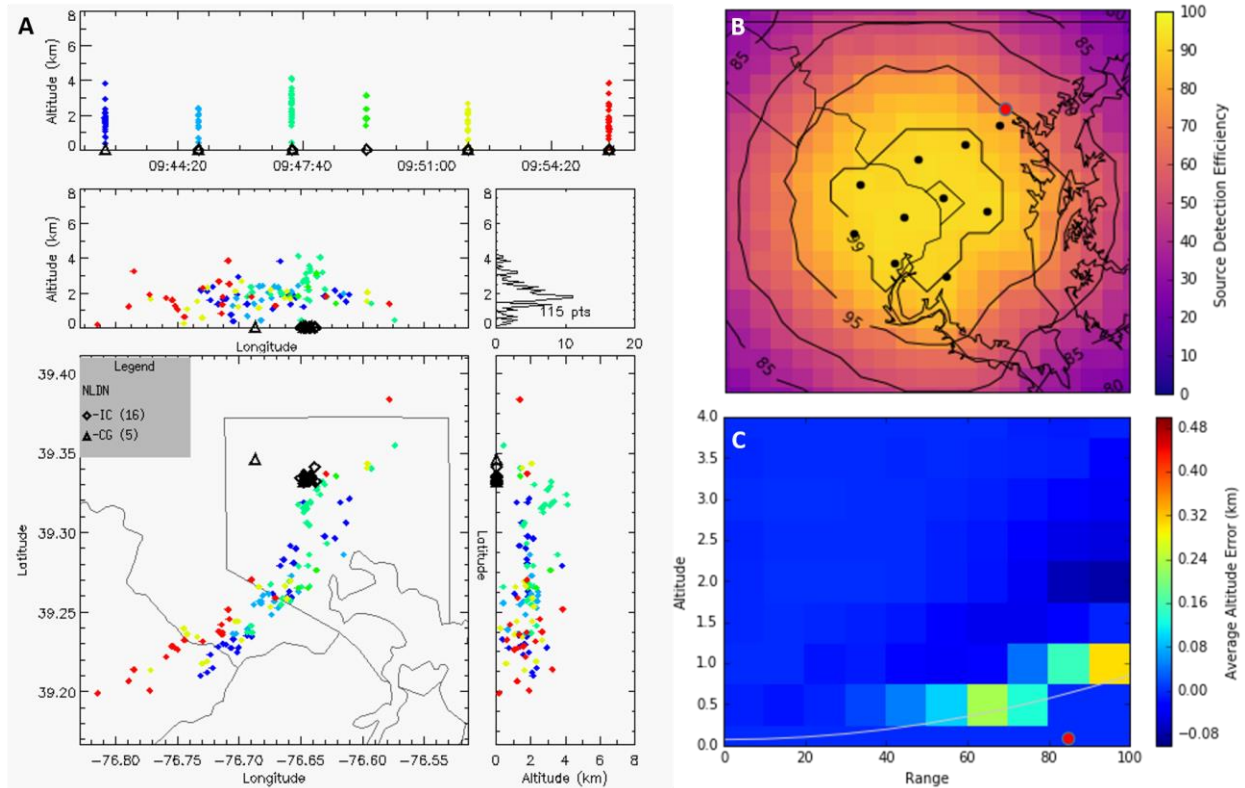


Figure 10 – The location of additional flash detections on 6 February 2010 for the DCLMA (Panel A), the source detection efficiency map for 6 February 2010 (Panel B), source altitude detection and altitude error on 6 February 2010 (Panel C). Panel A is the same as Fig. 1, but for LMA detections between 09:42:00 UTC through 09:57:00 UTC on 6 February 2010. In Panel B the black dots are the locations of sensors active during this event, the red dot is the location of the WBAL-TV communications tower responsible for initiating lightning flashes, and black contours are the source detection efficiency using the Chmielewski *and Bruning*, [2016] technique. In Panel C, shaded boxes indicate the average altitude error in km, and the grey line indicates the minimum detectable height of VHF sources using the DCLMA on this day, and the red dot is the location of the WBAL-TV communications tower.

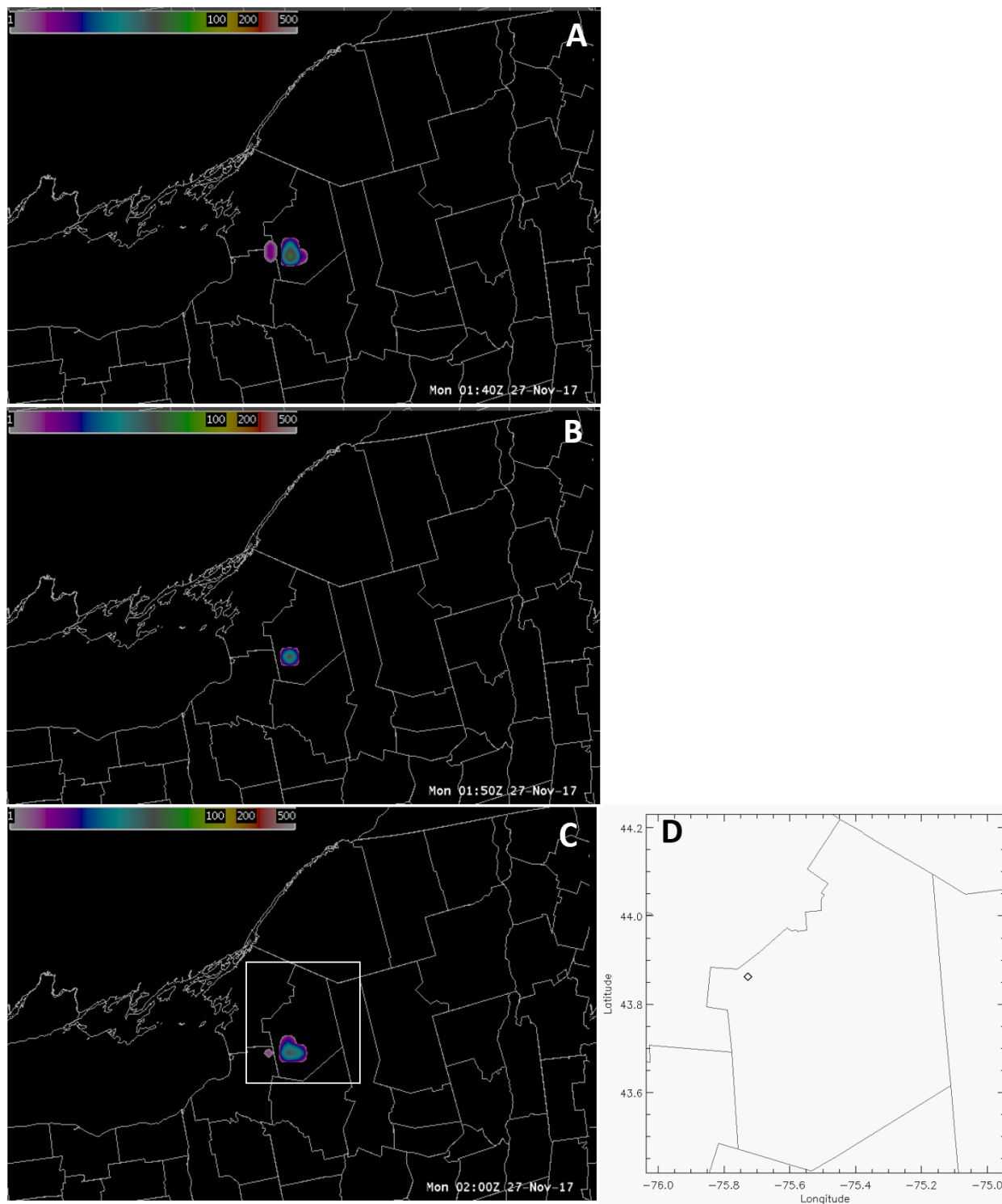


Figure 11. GLM event data from an electrified snowfall event on 27 November 2017. Panels A, B, and C are GLM event data within the National Weather Service's Advanced Weather Interactive Processing System version 2 (AWIPS2) using the NOAA GRB system to deliver

892 Level-2 GLM data. Panel A represents data from 0130 UTC up to 0140 UTC, Panel B  
893 represents data from 0140 UTC up to 0150 UTC, and Panel C represents data from 0150 UTC up  
894 to 0200 UTC. Panel D shows the location of all NLDN flashes between 0130 and 0200 UTC on  
895 27 November 2017. The white box in Panel C indicates the location of Panel D in the image and  
896 the black diamonds are the location of 8 –IC flashes all located at the same latitude and  
897 longitude.